ผลของด็อกโซรูบิซินต่อการแสดงออกของพี-ไกลโคโปรตีนในระหว่างการเปลี่ยนสภาพของเซลล์คาโค-ทูเป็นเซลล์เอนเทอโรไซต์

นายอุดมศักดิ์ อุดมนิโลบล

วิทยานิพนธ์นี้เป็นส่วนหนึ่งของการศึกษาตามหลักสูตรปริญญาเภสัชศาสตรมหาบัณฑิต
สาขาวิชาเภสัชวิทยาและพิษวิทยา ภาควิชาเภสัชวิทยาและสรีรวิทยา
คณะเภสัชศาสตร์ จุฬาลงกรณ์มหาวิทยาลัย
ปีการศึกษา 2558

THE EFFECT OF DOXORUBICIN ON P-GLYCOPROTEIN EXPRESSION DURING ENTEROCYTIC DIFFERENTIATION OF CACO-2 CELLS

Mr. Udomsak Udomnilobol

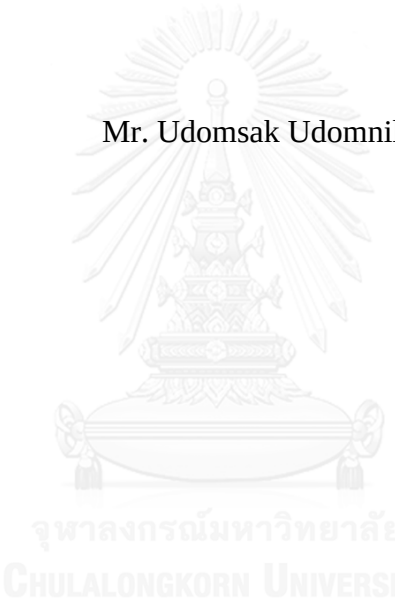

A Thesis Submitted in Partial Fulfillment of the Requirements
for the Degree of Master of Science in Pharmacy Program in Pharmacology and Toxicology
Department of Pharmacology and Physiology
Faculty of Pharmaceutical Sciences
Chulalongkorn University
Academic Year 2015

Thesis Title	THE EFFECT OF DOXORUBICIN ON P-GLYCOPROTEIN EXPRESSION DURING ENTEROCYTIC DIFFERENTIATION OF CACO-2 CELLS
By	Mr. Udomsak Udomnilobol
Field of Study	Pharmacology and Toxicology
Thesis Advisor	Associate Professor Suree Jianmongkol, Ph.D.

Accepted by the Faculty of Pharmaceutical Sciences, Chulalongkorn University in Partial Fulfillment of the Requirements for the Master's Degree

.....Dean of the Faculty of Pharmaceutical Sciences
(Assistant Professor Rungpetch Sakulbumrungsil, Ph.D.)

THESIS COMMITTEE

.....Chairman
(Assistant Professor Pornpimol Kijsanayotin, Ph.D.)
.....Thesis Advisor
(Associate Professor Suree Jianmongkol, Ph.D.)
.....Examiner
(Assistant Professor Rataya Luechapudiporn, Ph.D.)
.....External Examiner
(Assistant Professor Pathama Leewanich, Ph.D.)

อุดมศักดิ์ อุดมนิโลบล : ผลของด็อกโซรูบิซินต่อการแสดงออกของพี-ไกลโคโปรตีนในระหว่างการเปลี่ยนสภาพของเซลล์คาโค-ทูเป็นเซลล์เอนเทอโรไซต์ (THE EFFECT OF DOXORUBICIN ON P-GLYCOPROTEIN EXPRESSION DURING ENTEROCYTIC DIFFERENTIATION OF CACO-2 CELLS) อ.ที่ปรึกษาวิทยานิพนธ์หลัก: รศ. ภญ. ดร.สุรีย์ เจียรณ์มงคล, 68 หน้า.

เซลล์คาโค-ทูนำมาจากเซลล์มะเร็งลำไส้ใหญ่ที่มีการแสดงออกของพี-ไกลโคโปรตีน โดยระยะการเปลี่ยนสภาพของเซลล์อาจส่งผลต่อสภาวะรีดอกซ์ภายในเซลล์ การสร้างอนุมูลอิสระ และการตอบสนองต่อสารเคมีต่างๆ การศึกษานี้จึงมุ่งตรวจสอบอิทธิพลของระยะการเปลี่ยนสภาพของเซลล์คาโค-ทูต่อกระบวนการแปลรหัสของยีนเอบีซีบีวันที่ถูกเหนี่ยวนำด้วยด็อกโซรูบิซิน และความเกี่ยวข้องของอนุมูลอิสระต่ออิทธิพลดังกล่าว ในการศึกษานี้ระยะการเปลี่ยนสภาพของเซลล์คาโค-ทูถูกแบ่งเป็นสามระยะ ได้แก่ ก่อน ระหว่าง และหลังการเปลี่ยนสภาพ ซึ่งพบว่าสัดส่วนกลูต้าไธโอนในรูปรีดิวซ์ต่อรูปออกซิไดซ์เปลี่ยนเข้าสู่สภาวะรีดิวซ์มากขึ้นเมื่อเซลล์คาโค-ทูเกิดการเปลี่ยนสภาพ ผลการศึกษาพบว่าด็อกโซรูบิซินสามารถเปลี่ยนแปลงการแสดงออกของพี-ไกลโคโปรตีนในขั้นตอนการแปลรหัสได้ในทุกระยะการเปลี่ยนสภาพของเซลล์คาโค-ทู ระดับอนุมูลอิสระที่ถูกเหนี่ยวนำด้วยด็อกโซรูบิซินเพิ่มขึ้นอย่างมีนัยสำคัญเฉพาะเซลล์ในระยะก่อนการเปลี่ยนสภาพซึ่งมีสภาวะออกซิไดซ์มากกว่าเซลล์ในระยะอื่น ในเซลล์ระยะก่อนการเปลี่ยนสภาพนั้นพบว่าเอ็น-อะซิติลซีสเตอีนสามารถยับยั้งการเกิดอนุมูลอิสระได้อย่างสมบูรณ์และยับยั้งการเพิ่มระดับเอ็มอาร์เอ็นเอของยีนเอบีซีบีวันได้บางส่วน ในเซลล์ระยะระหว่างการเปลี่ยนสภาพพบว่าเอ็น-อะซิติลซีสเตอีนสามารถยับยั้งการเพิ่มระดับเอ็มอาร์เอ็นเอของยีนเอบีซีบีวันแต่มีผลยับยั้งเล็กน้อยต่อการลดระดับเอ็มอาร์เอ็นเอของยีนเอบีซีบีวันที่ถูกเหนี่ยวนำด้วยด็อกโซรูบิซิน ในเซลล์ระยะหลังการเปลี่ยนสภาพพบว่าเอ็น-อะซิติลซีสเตอีนไม่มีผลต่อการเพิ่มระดับเอ็มอาร์เอ็นเอของยีนเอบีซีบีวันที่ถูกเหนี่ยวนำด้วยด็อกโซรูบิซิน การศึกษานี้สรุปได้ว่าระยะการเปลี่ยนสภาพของเซลล์คาโค-ทูสามารถกำหนดผลของด็อกโซรูบิซินต่อระดับอนุมูลอิสระภายในเซลล์และการเปลี่ยนแปลงการแสดงออกของยีนเอบีซีบีวันได้ โดยอนุมูลอิสระอาจมีส่วนร่วมในการเปลี่ยนแปลงการแปลรหัสของยีนเอบีซีบีวันที่ถูกเหนี่ยวนำด้วยด็อกโซรูบิซินในเซลล์ระยะก่อนและระยะระหว่างการเปลี่ยนสภาพแต่ไม่มีส่วนร่วมในเซลล์ระยะหลังการเปลี่ยนสภาพ เป็นไปได้ว่าสภาวะรีดอกซ์ภายในเซลล์มีอิทธิพลต่ออนุมูลอิสระที่ถูกสร้างขึ้นจากด็อกโซรูบิซิน แต่อย่างไรก็ตามอนุมูลอิสระไม่ใช่กลไกเพียงอย่างเดียวในการเปลี่ยนแปลงระดับเอ็มอาร์เอ็นเอของยีนเอบีซีบีวันในแต่ละระยะการเปลี่ยนสภาพของเซลล์คาโค-ทู

ภาควิชา เภสัชวิทยาและสรีรวิทยา ลายมือชื่อนิสิต .....

สาขาวิชา เภสัชวิทยาและพิษวิทยา ลายมือชื่อ อ.ที่ปรึกษาหลัก .....

ปีการศึกษา 2558

5676228333 : MAJOR PHARMACOLOGY AND TOXICOLOGY
KEYWORDS: ABCB1 / CACO-2 / DOXORUBICIN / GLUTATHIONE / P-GLYCOPROTEIN / REACTIVE OXYGEN SPECIES / REDOX

UDOMSAK UDOMNILOBOL: THE EFFECT OF DOXORUBICIN ON P-GLYCOPROTEIN EXPRESSION DURING ENTEROCYTIC DIFFERENTIATION OF CACO-2 CELLS. ADVISOR: ASSOC. PROF. SUREE JIANMONGKOL, Ph.D., 68 pp.

Caco-2 cells are derived from human colon adenocarcinoma cells with an intrinsic expression of P-glycoprotein (P-gp). The differentiation phases might affect cellular redox status, reactive oxygen species (ROS) production, and cellular response to chemical threats. This study investigated the influence of the differentiation states of Caco-2 cells on cellular response at transcription level of *ABCB1* gene toward doxorubicin treatment and the involvement of ROS. In this study, the differentiation states of Caco-2 cells were divided into three phases including the pre-, during-, and post-differentiation. The GSH/GSSG ratio apparently shifted to a more reduced state when the cells differentiated. Doxorubicin could affect *ABCB1*/P-gp expression at transcription level in Caco-2 cells at all growth states. An intracellular ROS level was significantly increased by doxorubicin treatment only in the pre-differentiated cells, which had an apparently more oxidized state than the cells in other phases. In the pre-differentiated cells, a known antioxidant *N*-acetylcysteine (NAC) was able to entirely inhibit ROS production, and partially inhibited upregulation of *ABCB1* mRNA. In the during-differentiation phase, NAC potentially blocked doxorubicin-mediated upregulation of *ABCB1* mRNA, but it had little effect on doxorubicin-mediated downregulation. In the post-differentiation phase, NAC had no effect on doxorubicin-mediated *ABCB1* upregulation. In conclusion, the differentiation states of Caco-2 cells could determine the effect of doxorubicin on intracellular ROS level and *ABCB1* gene expression. The ROS might take part in the mechanism of doxorubicin-mediated *ABCB1* alteration at the transcription level in the pre- and the during-differentiation phases, but not in the post-differentiation state. It was likely that cellular redox status had an influence on ROS generated from doxorubicin. However, ROS was not the solely mechanism responsible for doxorubicin-mediated alteration of *ABCB1* mRNA in Caco-2 cells at each differentiation state.

Department: Pharmacology and Physiology Student's Signature .....
Field of Study: Pharmacology and Toxicology Advisor's Signature .....
Academic Year: 2015

ACKNOWLEDGEMENTS

Although only my name printed on the cover, many kind people have contributed their help and support to my thesis. I owe my gratitude to all those people listed on this section who have made this thesis becomes possible.

Firstly, I would like to express my sincere gratitude to my thesis adviser Associate Professor Suree Jianmongkol, Ph.D. for her patient, support, and encouragement. The door to her office was always opened whenever I ran into the troubles. Without her helps, I could not imagine how this thesis would be.

Beside my advisor, I am very grateful to thank Assistant Professor Nontima Vardhanabhuti, Ph.D. She devoted her valuable time to teach me how to do scientific research with etiquette and morality.

I would like to acknowledge my thesis committee, Assistant Professor Pornpimol Kitjsanayotin, Ph.D., Assistant Professor Rataya Luechapudiporn, Ph.D., and Assistant Professor Pathama Leewanich, Ph.D. for their suggestions and comments.

I would like to express my appreciation to Associate Professor Kanokporn Triwitayakorn, Ph.D. and her research team of the Institute of Molecular Bioscience, Mahihol University. The knowledge about techniques in molecular biology that they taught me was expanded to this thesis.

I would like to thank Niwed Kullawong, Ph.D. of the School of Health Science, Mae Fah Luang University for giving me the first step in quantitative PCR technique.

I owe my gratitude to Piyanuch Wonganan, Ph.D. and Ms. Nanthanat Virattana of the Faculty of Medicine, Chulalongkorn University for their help when gene expression analysis was established for the first time in my laboratory.

I would like to express my thankful to Mr. Noppadol Sa-Ard-Iam of the Immunology Laboratory, Faculty of Dentistry, Chulalongkorn University for his guides about flow cytometry.

I sincerely thank to Mr. Nonthaneth Nalinratana for teaching me how to do the SDS-PAGE and western blot analysis.

I would like to acknowledge the Scholarship from the Graduate School, Chulalongkorn University to commemorate 72nd Anniversary of his Majesty King Bhumibol Adulyadej and the 90th Anniversary Chulalongkorn University Fund (Ratchadaphiseksomphot Endowment Fund).

I also thank the Microbiology, Molecular Biology, and Biotechnology (MMBB) Research Unit of the Chulalongkorn University Drug and Health Products Innovation & Promotion Center (CU.D.HIP) for all facility.

I thank to all members of the Department of Pharmacology and Physiology, Faculty of Pharmaceutical Sciences, Chulalongkorn University for providing me with all necessary facility.

Finally, I also thank my family, friends, and others for their unceasing encouragements.

CONTENTS

Page

LIST OF FIGURES

LIST OF TABLES

LIST OF ABBREVIATIONS

ABCB1	=	ATP-binding cassette subfamily B member 1 gene
ALP	=	alkaline phosphatase enzyme
ATP	=	adenosine triphosphate
bps.	=	base pairs
cDNA	=	complementary DNA
C_q	=	quantification cycle
CV	=	coefficient of variation
CYP450	=	cytochrome P450
DMEM	=	Dubecco's modified Eagle's media
DMSO	=	dimethylsulfoxide
DNA	=	deoxyribonucleic acid
DNase	=	deoxyribonuclease enzyme
dNTP	=	deoxynucleotide
Dox	=	doxorubicin
DTNB	=	5,5-dithio-bis-(2-nitrobenzoic acid) or Ellman's reagent
EDTA	=	ethylenediaminetetraacetic acid
FITC	=	fluorescein isothiocyanate
GAPDH	=	glyceraldehyde 3-phosphate dehydrogenase gene
GAPDH	=	glyceraldehyde 3-phosphate dehydrogenase protein
GSH	=	reduced glutathione
GSH/GSSG	=	reduced-to-oxidized glutathione
GSSG	=	oxidized glutathione
GS-TNB	=	glutathione-2-nitro-5-thiobenzoate
mRNA	=	messenger RNA
NaBT	=	sodium butyrate
NAC	=	*N*-acetylcysteine
NADH	=	nicotinamide adenine dinucleotide
NADPH	=	nicotinamide adenine dinucleotide phosphate
PBS	=	phosphate buffer saline
PCR	=	polymerase chain reaction
P-gp	=	P-glycoprotein
qPCR	=	quantitative PCR or real-time PCR
RNA	=	ribonucleic acid
ROS	=	reactive oxygen species
RT-qPCR	=	reverse transcriptase-quantitative PCR
SEM	=	standard error of the mean
TNB	=	2-nitro-5-thiobenzoate

CHAPTER I
INTRODUCTION

Background and rationales

P-glycoprotein (P-gp) is an efflux drug transporter belonged to the ATP-binding cassette (ABC) superfamily. It is encoded from *ABCB1* gene and expressed in several organs including the brush border membrane of small intestine (Lin and Yamazaki, 2003a). The mechanisms of P-gp expression involve with several orchestrated signaling pathways, especially those activated by stress signals. For example, hydrogen peroxide could affect the expression level of *ABCB1* mRNA in Caco-2 cells (Terada et al., 2014). Hence, it has been hypothesized that upregulation of P-gp expression may be a cellular survival mechanism in response to stresses.

Caco-2 cells are derived from human colon adenocarcinoma cells with an intrinsic expression of P-gp. After confluency, Caco-2 cells undergo spontaneous differentiation to the polarized enterocyte-like monolayers expressing brush border enzymes such as alkaline phosphatase and sucrase isomaltase (Ding et al., 1998). Several chemicals such as capsaicin, curcuminoid, doxorubicin, lipopolysaccharide, nitric oxide donors, nonsteroidal anti-inflammatory drugs, piperine, and venlafaxine were able to alter P-gp expression either in the confluent pre-differentiated or in the fully differentiated Caco-2 cells (Hou et al., 2008, Silva et al., 2011, Duan et al., 2012, Ehret et al., 2007, Han et al., 2006, Han et al., 2008, Takara et al., 2009, Mishra et al., 2008). However, there is no clear evidence to suggest the influence of Caco-2 growth states on chemical-induced P-gp upregulation. Regarding to this, the characteristics of cells in each growth state might have significant contribution to different responses toward chemical treatment. It was reported that Caco-2 cells had the reduced glutathione (GSH) decreased gradually during enterocytic differentiation whereas the oxidized form (GSSG) remained unchanged. This finding suggested that cellular redox status shifted toward a more oxidized state, as indicated by a decrease in GSH/GSSG ratio (Nkabyo et al., 2002). As known, glutathione is a major redox buffering system counteracting an elevation of reactive oxygen species (ROS). It was

possible that an increase of ROS could disrupt redox balance in the differentiated cells more than that in the pre-differentiated cells.

Doxorubicin is an anthracycline antibiotic with P-gp induction capability in several cancer cells such as MCF-7, Caco-2, and LoVo cells (Liu et al., 2014, Bertram et al., 1996, Ma et al., 2012). It was reported that doxorubicin rapidly upregulated P-gp level in the confluent pre-differentiated Caco-2 cells in the concentration- and time-dependent manners. Treatment the cells with doxorubicin at the concentration up to 100 μM for 6 hours significantly increased an expression level of P-gp. Moreover, an increase of P-gp expression was more pronounced when the treatment time with doxorubicin increased from 6 to 24 hours (Silva et al., 2011). Nevertheless, there is no evidence indicated that doxorubicin could affect P-gp expression in other growth states of Caco-2 cells. In addition, it was demonstrated that doxorubicin at the concentration of 3 μM could induce an increase of ROS level and P-gp expression in HepG2 cells. Pretreatment these cells with ursodeoxycholic acid (100 μM) prior to doxorubicin could suppress ROS production and inhibit an increase of P-gp expression level (Komori et al., 2014). These findings suggested the possible involvement of ROS in P-gp upregulation induced by doxorubicin. Taken together, it was possible that doxorubicin-mediated expression of P-gp was determined by the differentiation states of Caco-2 cells. The differentiated cells might be more sensitive to doxorubicin-mediated alteration of P-gp expression than the cells in other growth states.

Therefore, this study investigated the effect of doxorubicin on *ABCB1*/P-gp expression in each differentiation state of Caco-2 cells. The influence of growth states toward doxorubicin treatment on *ABCB1*/P-gp expression was determined and correlated to cellular redox status.

Hypotheses

Doxorubicin was able to alter *ABCB1*/P-gp expression in Caco-2 cells through ROS-mediated mechanisms. It was likely that doxorubicin could increase *ABCB1*/P-gp expression at the higher degree in the cells with higher oxidized redox status.

Objectives

The objectives of this study were

1. To investigate the effect of doxorubicin on *ABCB1*/P-gp expression in each differentiation state of Caco-2 cells.
2. To identify the differentiation states in which *ABCB1*/P-gp expression was affected by doxorubicin treatment.
3. To determine an involvement of ROS and cellular redox status on doxorubicin-mediated *ABCB1*/P-gp alteration in each differentiation state of Caco-2 cells.

Conceptual framework

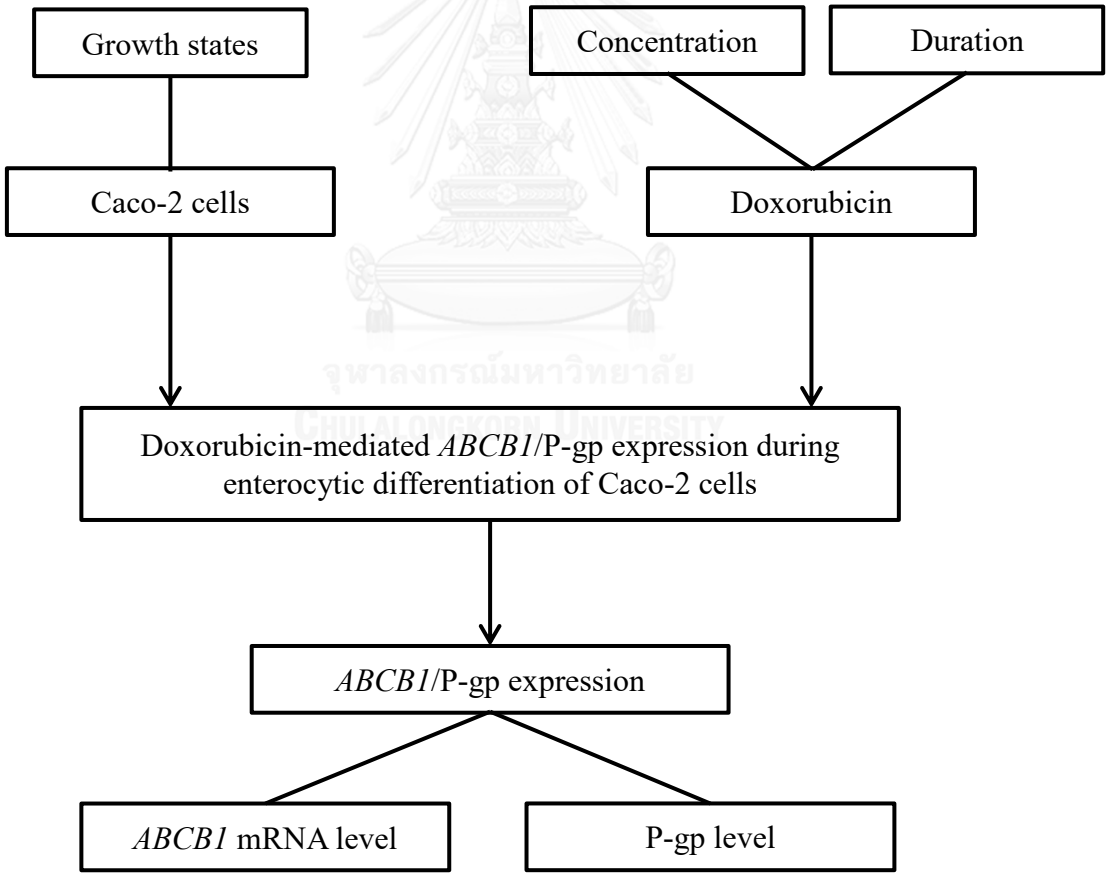

CHAPTER II
LITERATURE REVIEWS

P-glycoprotein

P-glycoprotein (P-gp) is a 170-kDa integral membrane protein in the ATP-binding cassette (ABC) superfamily. P-gp functions as an ATP-dependent drug efflux pump with broad substrate specificity. Drugs in various classes have been identified as P-gp substrates, for example, cardiac glycoside (e.g. digoxin), protease inhibitors (e.g. indinavir), immunosuppressive agents (e.g. cyclosporine A), and anticancer drugs (e.g. vinblastine, doxorubicin, and etoposide) (Lin and Yamazaki, 2003b). With an energy provided from ATP hydrolysis, P-gp pumps the substrate out of the cells against the concentration gradient. Therefore, this protein is a gate-keeper protecting the cells from chemical insults through limiting cellular accumulation of cytotoxic agents.

P-gp is ubiquitously expressed in human tissues including colon, liver, kidney, blood-brain barrier, blood-testis barrier, and placenta (Lin and Yamazaki, 2003b). It is encoded from an ATP-binding cassette subfamily B member 1 (*ABCB1*) gene. This gene has a TATA-less promoter, but contains multiple transcription factor start sites including inverted CCAAT (Y-box), CCAAT box motif, and GC-box elements (Labialle et al., 2002, Sundseth et al., 1997). These transcription factors promote an assembly of RNA polymerase II that initiates the *ABCB1* transcription. Then, *ABCB1* mRNA is translated and folded into the 150-kDa intermediate P-gp in endoplasmic reticulum. The maturation to be 170-kDa P-gp occurs in golgi apparatus by several glycosylation steps (Fu and Arias, 2012). The fully matured P-gp is subsequently delivered to the cell surface via two pathways including cytoskeleton facilitating and endosomal pathways (Fu and Arias, 2012). In addition to plasma membrane, P-gp is found to localize in other subcellular compartments such as nuclear membrane, mitochondria, and lysosomes (Szaflarski et al., 2013, Shen et al., 2012, Yamagishi et al., 2013). The degradation of P-gp is mainly mediated through lysosomal degradation pathway (Katayama et al., 2015). Either an alteration in synthesis or degradation could affect expression level of P-gp.

Transcriptional rate of *ABCB1* gene is affected by a numerous transcription factors including Sp1, YB-1, heat shock factor-1, NF-κB, p53, etc. (Labialle et al., 2002, Katayama et al., 2014). Most of these transcription factors such as NF-κB are commonly activated in response to cellular stresses (Morgan and Liu, 2011). Therefore, it is possible that P-gp expression can be altered by cellular stresses including heat shock (Vilaboa et al., 2000), osmotic pressure (Miyazawa et al., 2007), endoplasmic reticulum stress (Ledoux et al., 2003), and oxidative stress (Hartz et al., 2008). For example, treatment rat brain endothelial cells with *l*-buthionine-(*S,R*)-sulfoximine (BSO) at the concentration of 200 μM for 24 hours caused an increase of P-gp expression (Hong et al., 2006). In addition, various anticancer drugs were reported to affect expression of P-gp. For example, vincristine showed the biphasic modulation of *ABCB1* mRNA expression in Caco-2 cells. At 48-hour treatment, vincristine at the concentrations of 5 and 10 nM decreased *ABCB1* mRNA level, whereas 1,000 and 2,000 nM increased *ABCB1* mRNA expression significantly (Huang et al., 2006). Some anticancer drugs such as doxorubicin, geldanamycin, and 5-fluorouracil can directly and indirectly induce cellular stresses (Gorrini et al., 2013). Therefore, a few studies hypothesized that an increase of P-gp expression is a survival response against cellular stresses.

The number of P-gp showing up on the cell surface could determine an entry of P-gp substrates into the cells. There was a study showing the effect of expression level of P-gp on the cellular permeability of P-gp substrate drugs (i.e. digoxin, quinidine, verapamil, and vinblastine). The V_{max} and K_m values of P-gp-mediated efflux for these drugs had a strong linear correlation with the differential expression level of P-gp in Caco-2, P-gp-induced Caco-2, P-gp-highly induced Caco-2, MDR1-knockdown Caco-2, and MDCKII-MDR1 cells (Shirasaka et al., 2008). Therefore, the potential of drug and natural compounds to alter P-gp expression has been an important issue needed to study.

Caco-2 cells

Caco-2 cells are derived from human colon adenocarcinoma cells which exhibit both colonic and enterocytic phenotypes (Engle et al., 1998). This cell line expresses various efflux drug transporters including P-gp. The remarkable feature of

this cell line is a potential to differentiate either by long-term culturing or differentiation inducers.

Spontaneous differentiation

Caco-2 cells are the only cell line of human colon cancer cells exhibiting the spontaneous differentiation with the mature enterocytic phenotypes (Chantret et al., 1988). After culturing over confluence, Caco-2 cells undergo G_1 arrest and spontaneously differentiate to form a polarized enterocyte-like monolayer expressing apical brush border enzymes such as alkaline phosphatase and sucrase-isomaltase (Ding et al., 1998). The transition from proliferative to differentiated cells is found to regulate through homeobox protein CDX2. The cellular level of CDX2 is very low in undifferentiated cells, but increases abundantly after reaching confluency. The more CDX2 protein is able to bind strongly to DNA elements which are the genes necessary for differentiation process (Boyd et al., 2010).

The characteristics of Caco-2 cells may gradually change in relation to their culturing period. Generally, Caco-2 cells are grown into sequential phases including proliferation, pre-differentiation, during-differentiation and fully differentiation (Sambuy et al., 2005). These growth states can be specified by a number of differentiation markers. The differentiation markers can be either those for proliferative cells or for specific differentiated cells. The markers for proliferative cells relate to cell division process such as number of the cells, percentage of cells in each cell cycle phase, rate of DNA synthesis (either bromodeoxyuridine or thymidine incorporation), expression level of cell cycle proteins, etc. (Leoni et al., 2012, Goto et al., 2003, Ding et al., 1998). The specific markers of enterocytic phenotypes can be used to specify the differentiated Caco-2 cells. The early differentiation can be determined by CDX2 expression, localization, and other CDX2 responsive gene products (Boyd et al., 2010, Natoli et al., 2013). Subsequently, the differentiated Caco-2 cells can be identified by expression and activity of brush border enzymes (alkaline phosphatase, alanine aminopeptidase, and sucrase-isomaltase) (Ferruzza et al., 2012b). In addition, the phenotypes of polarized epithelial cells can be used as differentiation markers, for example, microvilli and tight junction formation (Ferruzza et al., 2012a, Aggarwal et al., 2011).

Cellular redox status can be altered in relation to the differentiation phases of the cells (Watson et al., 2003). It was reported that reduced glutathione (GSH) decreased gradually during enterocytic differentiation of Caco-2 cells whereas an oxidized glutathione (GSSG) remained unchanged. However, the redox status of thioredoxin did not change during Caco-2 differentiation (Nkabyo et al., 2002). Glutathione is a redox buffering system which is the most abundant in the cells when compares to other systems such as nicotinamide adenine dinucleotide (NADH), nicotinamide adenine dinucleotide phosphate (NADPH), and thioredoxin systems (Schafer and Buettner, 2001). In addition, the reduced-to-oxidized glutathione (GSH/GSSG) ratio is generally used as a parameter for cellular redox status. The higher GSH/GSSG ratio reflects more reduced status of the cells and vice versa (Schafer and Buettner, 2001, Flohe, 2013). This finding suggested that cellular redox status shifted toward a more oxidized state when Caco-2 cells underwent differentiation.

The expression of efflux drug transporters especially P-gp varies regarding to the spontaneous differentiation of Caco-2 cells. It was reported that an expression level of both *ABCB1* mRNA and P-gp in Caco-2 cells was the highest at the pre-confluent state, and then reduced gradually regarding to cell differentiation. The regulation of *ABCB1* mRNA expression at the pre-confluent state was mainly through mRNA stability rather than its transcription rate (Goto et al., 2003). In contrast, another study demonstrated that expression of *ABCB1* mRNA was higher in the differentiated cells than in the undifferentiated cells (Siissalo et al., 2007). Therefore, a culture-period dependent expression of P-gp remained unclear.

The expression of P-gp could be affected by several drugs and natural substances. In Caco-2 cells, the capability of tested compounds on P-gp expression is conducted in two distinct cell states including the confluent pre-differentiated and the fully differentiated cells. The compounds such as curcuminoid, doxorubicin, nitric oxide donors, and venlafaxine were found to change P-gp expression in the confluent Caco-2 cells (Hou et al., 2008, Silva et al., 2011, Duan et al., 2012, Ehret et al., 2007). Alternatively, it was reported that capsaicin, piperine, nonsteroidal anti-inflammatory drugs, and lipopolysaccharide were capable to change P-gp expression in the differentiated Caco-2 cells (Han et al., 2006, Han et al., 2008, Takara et al., 2009,

Mishra et al., 2008). Until now, there has been no study comparing the effect of the same compound on P-gp expression at various differentiation states of Caco-2 cells.

Substance-induced differentiation

Caco-2 differentiation can be accelerated by several substances including short-chain fatty acids, cell culture surface, and specific types of culture media (Liang et al., 2000, Deng et al., 2013, Malago et al., 2003). Among differentiation inducers, sodium butyrate (NaBT) is the most well-known differentiation inducer published in Caco-2 cells. Treatment the cells with NaBT accelerates Caco-2 differentiation as indicated by an increase of brush border enzyme activities, tight junction formation, and transepithelial electrical resistance (Peng et al., 2007). The mechanisms of NaBT-induced differentiation are proposed to occur via multiple signaling pathways including vitamin D receptor, protein kinase C, and c-Jun N-terminal kinase (JNK) pathways (Gaschott et al., 2001, Orchel et al., 2005). In addition, it was reported that NaBT induced differentiation in simultaneous with apoptosis in Caco-2 cells (Ruemmele et al., 2003). However, the effects of NaBT on both differentiation and apoptosis could be shunted when Caco-2 cells enter their spontaneous differentiation (Mariadason et al., 2001).

Similar to spontaneous differentiation, the cellular redox regulation is changed after NaBT-induced differentiation. As shown, Caco-2 cells treated with NaBT (4 mM, 24 hours) showed a 5-fold decrease in the ratio of NADPH/NADP which is one of cellular redox buffering system (Blouin et al., 2011). In addition, NaBT (10 mM) increased superoxide dismutase activity, but decreases glutathione peroxidase activity by 2 folds (Orchel et al., 2006). However, there is no study reported the relationship between NaBT and cellular glutathione level in Caco-2 cells. In HT-29 colon cancer cells, NaBT-induced differentiation resulted in a decrease of cellular glutathione level in both GSH and GSSG. The effect was more pronounced when the cells were cotreated with NaBT and glutathione synthesis inhibitor, *l*-buthionine-(*S,R*)-sulfoximine (BSO) (Benard and Balasubramanian, 1997). These data suggested a possible involvement of cellular redox status in NaBT-induced differentiation.

The P-gp expression in NaBT-treated Caco-2 cells has studied very little. Previous study reported that treatment of NaBT (4 mM) for 24 hours increased an expression level of P-gp in CYP3A4-transfected Caco-2 cells (Cummins et al., 2001). Thus, NaBT itself could upregulate P-gp expression in Caco-2 cells. However, there has been no study conducting P-gp induction experiment in NaBT-induced differentiated Caco-2 cells.

Doxorubicin-mediated alteration of P-glycoprotein expression

Doxorubicin (or adriamycin) is an anthracycline antibiotic with the cytotoxic effect against several cancer cells including breast cancer, acute myeloid leukemia, multiple myeloma, etc. (Thorn et al., 2011). In addition to cytotoxic activity, doxorubicin has a capability to increase *ABCB1*/P-gp expression. In an *in vitro* cell culture model, doxorubicin increases P-gp expression through selection and induction processes. In the selection process, the cells were cultured and maintained in the doxorubicin-containing media in order to exclude the death cells. As known, doxorubicin is a P-gp substrate and can lose its effectiveness in *ABCB1*-overexpressed cells. Hence, the cells with high P-gp expression level will survive doxorubicin treatment (Liu et al., 2014, Ma et al., 2012). Furthermore, it was reported that the expression of P-gp could be upregulated in various cell culture models after both transient and long-term treatment with doxorubicin. For example, doxorubicin and other anthracycline antibiotics including daunorubicin and epirubicin significantly induced *ABCB1* mRNA expression within 4 hours of drug exposure in T-cell lymphoblastic leukemia. Neither vinblastine nor vincristine had an inductive effect on *ABCB1* expression in this cell line (Hu et al., 1995). The effect of doxorubicin on P-gp expression was also reported in clinical studies. Rapid *ABCB1* mRNA upregulation was observed in tumor biopsies obtained from the patients with metastatic sarcoma at 20 min after lung infusion of doxorubicin (Abolhoda et al., 1999).

In addition to cancerous cells, doxorubicin was reported to induce P-gp expression in normal cells. It was demonstrated that single dose treatment with doxorubicin at 20 mg/kg significantly increased P-gp expression in cardiac tissues of C57Bl/10 mice at day 5 after dosing. In addition, P-gp expression was upregulated in

HL-1 cardiomyocytes after treatment with doxorubicin at the concentration of 333 nM for 36 hours (Budde et al., 2011). Exposure to doxorubicin at the concentration of 0.5 μg/ml for 8 hours specifically induced P-gp expression in rat liver cells, whereas expression of CYP450 remained unchanged. An inductive effect of doxorubicin on rat hepatic P-gp expression was inhibited by actinomycin D, suggesting that doxorubicin mediated P-gp induction at transcription level (Fardel et al., 1997). Furthermore, the pharmacokinetic profile of doxorubicin was changed after single dose of intravenous doxorubicin injection (6 mg/kg) to Balb/c mice. The area under the curve (AUC) of doxorubicin decreased by 2.3 folds following the second treatment because of an elevated level of P-gp in liver and small intestine (Gustafson and Long, 2001).

Taken together, doxorubicin is a potent P-gp inducer which can cause rapid induction of P-gp expression level in both normal and cancer cells. However, there is no evidence indicating that doxorubicin could downregulate P-gp expression.

The mechanism of doxorubicin-induced P-gp expression is still unclear. Doxorubicin can generate reactive oxygen species (ROS) and produce intracellular oxidative stress (Thorn et al., 2011). It was demonstrated that exposure with doxorubicin at the concentration of 3 μM could induce an increase of ROS level and P-gp expression in HepG2 cells. Pretreatment these cells with ursodeoxycholic acid (100 μM) prior to doxorubicin could suppress ROS production and inhibit an increase of P-gp expression level (Komori et al., 2014). These findings suggested the possible involvement of ROS in P-gp upregulation. In addition, tetrandrine prevented doxorubicin-mediated P-gp upregulation in K652 leukemic cells possibly through counteracting NF-κB signaling pathway (Shen et al., 2010). As known, the activation of NF-κB signaling cascade occurs in response to oxidative stress (Morgan and Liu, 2011). Moreover, it was shown that ROS generated from diesel exhaust particles enhanced P-gp expression at blood brain barrier in rat through oxidative stress-JNK-AP-1 cascade (Hartz et al., 2008). Hence, it is likely that the effect of doxorubicin on P-gp upregulation is mediated through mechanisms involving with ROS and oxidative stress. However, there are a number of studies indicating that ROS could cause downregulation of P-gp expression as well (Wartenberg et al., 2005,

Wartenberg et al., 2001). For example, ROS was capable to downregulate an intrinsic expression of P-gp in prostate tumor spheroids (Wartenberg et al., 2001).

Therefore, doxorubicin was used in this study as a P-gp inducer with a ROS generating property.

CHAPTER III
MATERIALS AND METHODS

Materials and instruments

I. Chemicals and reagents

2-Vinylpyridine, *β*-NADPH, Bradford reagent, DTNB (Ellman's reagent), glutathione (oxidized form), glutathione reductase from baker's yeast (*S. cerevisiae*), MEM nonessential amino acid, menadione sodium bisulfite, *N*-acetylcysteine, neutral red, paraformaldehyde, penicillin G potassium salt, *p*-nitrophenol, *p*-nitrophenyl phosphate, propidium iodide, protease inhibitor cocktail, sodium butyrate, streptomycin sulfate, and sulfosalicylic acid were purchased from Sigma Aldrich (St. Louis, MO, USA).

ABCB1 and *GAPDH* specific primers were synthesized by Integrated DNA Technologies Pte. Ltd. (The Gemini Singapore Science Park II, Singapore).

Anti-rabbit IgG, HRP-linked antibody, GAPDH (D16H11) XP® rabbit mAb, and MDR1/ABCB1 (E1Y7B) rabbit mAb were purchased from Cell Signaling Technology Inc. (MA, USA).

CellROX® deep red reagent, Pierce™ BCA protein assay kit, ribonuclease A, SuperSignal® west pico chemiluminescent substrate, TRIzol® reagent, SYBR Safe DNA gel stain, and TURBO DNA-free™ kit were purchased from Thermo Fisher Scientific Inc. (MA, USA).

Doxorubicin HCl and Triton® X-100 was purchased from Merck Millipore (Darmstadt, Germany).

Dubecco's modified Eagle medium (DMEM) and L-glutamine were purchased from Gibco Life Technologies (Grand Island, NY, USA).

Fetal bovine serum (FBS) was purchased from Biochrom AG (Berlin, Germany).

FITC mouse anti-human P-gp Ab was purchased from BD Biosciences (San Jose, CA, USA).

Improm-II™ reverse transcription system was purchased from Promega Corporation (WI, USA).

Precision plus protein™ dual color standards and SsoFast™ EvaGreen® Supermix were purchased from Bio-Rad Laboratories Inc. (CA, USA)

II. Experimental instruments

i. Flow cytometer: BD FACSCalibur (BD biosciences, CA, USA)
ii. Humidified CO_2 incubator: 3164 (Forma Scientific, OH, USA)
iii. Inverted light microscope: Axiovert 135 (Zeiss, Konstanz, Germany)
iv. Laminar air flow hood (HEPACO)
v. Luminescent image analyzer: ImageQuant LAS4000 (FUJIFILM corporation, Tokyo, Japan)
vi. Microplate reader: Wallac 1420 (Perkin Elmer Inc., MA, USA)
vii. Nanodrop: 2000 (Thermo Fisher Scientific Inc., MA, USA)
viii. Real-time PCR: CFX96™ Real-Time PCR Detection System (Bio-Rad Laboratories Inc., CA, USA)

Methods

I. Cell culture

The human colorectal adenocarcinoma cells (Caco-2, HTB-37™) were obtained from American Type Culture Collection (ATCC, Mannassas, VA, USA). Cells were maintained in DMEM containing 10% heat-inactivated FBS, 1% penicillin G/streptomycin, 1% non-essential amino acid, and 2 mM L-glutamine at 37°C in humidified atmospheric condition of 95% O_2 and 5% CO_2. The cells were routinely subcultured at approximately 70% confluency every 3-4 days.

Doxorubicin treatment: Caco-2 cells were seeded at the density of 20,000 cells/cm^2. The cells were treated with doxorubicin at the non-cytotoxic concentration for 24 hours. In some experiments, *N*-acetylcysteine (NAC 5 mM) was added in the medium 30 min prior to addition of

doxorubicin (Noda et al., 2001). At the end of treatment with doxorubicin, the cells were washed three times with phosphate buffer saline (PBS), and collected for further measurement.

In another experimental setting, the confluent Caco-2 cells were treated with sodium butyrate (NaBT, 2 mM) for another 2 days in order to induce differentiation (Wolter and Stein, 2002, Mariadason et al., 2001). Subsequently, the NaBT-treated cells were washed and treated with doxorubicin as mentioned above.

II. Determination of the differentiation phase of Caco-2 cells

In order to identify the differentiation phase of Caco-2 cells, percentage of cells in each cell cycle phase, total cell numbers, and alkaline phosphatase (ALP) activity were determined every 2 days after seeding up to 21 days.

i. Cell cycle analysis

The cells were fixed in 70% ethanol and stained with propidium iodide (20 μg/mL) at 37°C for 15 min. The fluorescent intensity of propidium iodide was measured by BD FACSCalibur flow cytometer at 488 and 585/42 nm for excitation and emission wavelengths, respectively. The percentage of cells in each cell cycle phase was gated from 10,000 events.

ii. Determination of cell numbers

The cells were trypsinized and resuspended in complete DMEM. The total cells were counted on hemocytometer.

iii. Determination of ALP activity

The cells were collected and homogenized in 10 mM Tris/150 mM NaCl buffer (pH 8.0). The cell homogenate (250 μL) was incubated with 2.5 mg/mL *p*-nitrophenyl phosphate (750 μL) at 37°C for 5 min, followed by addition of 0.5 M NaOH (50 μL) (Mariadason et al., 2001, Ferruzza et al., 2012b). The amount of *p*-nitrophenol was measured by spectrophotometry at 405 nm.

III. Assay for cell viability

Cell viability was determined by a neutral red uptake assay. The cells were incubated with neutral red solution (40 μg/mL) for 2 hours, and washed once with PBS. Then, the cells were treated with acidified ethanol (1% acetic acid in 50% ethanol) in order to extract intracellular neutral red. The amount of neutral red in the cell extract was quantified by spectrophotometer at 544 nm. The data was expressed as a percentage of solvent control group (0.5% DMSO). In this study, the non-cytotoxic concentration of doxorubicin was defined as the concentrations that produce cell viability of greater than 80%.

IV. Reverse transcriptase-quantitative polymerase chain reaction (RT-qPCR)

The effect of doxorubicin on *ABCB1* mRNA level during enterocytic differentiation of Caco-2 cells was determined by RT-qPCR. Briefly, total RNA was extracted from the cells with TRIzol reagent and digested residual DNA with TURBO DNA-free kit. Total RNA (250 ng) was reverse-transcribed with oligo $(dT)_{15}$ primer using Improm-II reverse transcription system. The PCR reaction was performed using SsoFast™ EvaGreen® Supermix on CFX™96 Real-time PCR Detection System from 1 μL of cDNA. The reaction was run for 40 cycles of 95°C 5 sec and 60°C 5 sec by using *ABCB1* primer (400 nM) or *GAPDH* primer (300 nM) (Konig et al., 2010, Wang et al., 2013). The specificity of amplified products was determined by melting curve analysis. Relative quantification was carried out by the Pfaffl's method (Pfaffl, 2001)

Gene	Sequences (5' → 3')	Product size
ABCB1 (NM_000927.4)	F: CCCATCATTGCAATAGCAGG R: TGTTCAAACTTCTGCTCCTGA	158 bps
GAPDH (NM_001256799.2)	F: TGCACCACCAACTGCTTAGC R: GGCATGGACTGTGGTCATGAG	87 bps

V. Western blot analysis

The effect of doxorubicin on P-gp level during enterocytic differentiation of Caco-2 cells was determined by western blot analysis.

Briefly, the cells were lysed with radioimmunoprecipitation assay (RIPA) buffer containing protease inhibitor cocktail. The protein lysate (20 μg) was run on sodium dodecyl sulfate-polyacrylamide gel electrophoresis (SDS-PAGE). The proteins were subsequently transferred to polyvinylidene fluoride (PVDF) membrane and blotted with MDR1/ABCB1 (E1Y7B) rabbit mAb (1:1000) and GAPDH (D16H11) XP® rabbit mAb (1:5000). Then, the blots were further incubated with Anti-rabbit IgG, HRP-linked antibody (1:2000) and developed using the SuperSignal® west pico chemiluminescent substrate under ImageQuant LAS4000 luminescent image analyzer. The band intensity was normalized to that of GAPDH with the use of Image J software (NIH, MA, USA).

VI. Determination of surface P-gp expression

The expression level of P-gp on the cell surface was determined by flow cytometry. Briefly, the cells were trypsinized at 37°C and resuspended in ice-cold PBS. The cells in antibody-labeled group were incubated with fluorescein isothiocyanate (FITC)-conjugated anti-human P-gp antibody in the dark at 4°C for 30 min. They were subsequently washed with ice-cold PBS containing 2% FBS and fixed with 1% paraformaldehyde in PBS. The cells in the unlabeled group were collected and fixed using similar processes as mentioned above, except that they were not treated with the FITC-conjugated antibody. The intensity of FITC fluorescence was measured by BD FACSCalibur flow cytometer at 488 and 530/30 nm for excitation and emission wavelengths, respectively. The fluorescent intensity of 10,000 events was used for data analysis.

VII. Determination of glutathione

The GSH/GSSG ratio was determined by the enzymatic recycling assay (Rahman et al., 2006). In brief, the cells were lysed with ice-cold extraction buffer (0.1% Triton-X and 0.6% sulfosalicylic acid in potassium phosphate-EDTA buffer). For measurement of total glutathione, the cell extract (20 μL) was incubated with the 120 μL equal mixture of glutathione reductase (3.33 units/mL) and DTNB (1.62 mM) at 25°C for 30 sec in order

to form GS-TNB adduct. Then, β-NADPH (0.8 mM, 60 µL) was added into the mixture to activate the reductase activity. The TNB would be released from the GS-TNB adduct and could be read its absorbance at 405 nm. For measurement of GSSG, the cell extract (100 µL) was incubated with 2-vinylpyridine (0.9 M, 2 µL) at room temperature for 1 hour. Then, the residual 2-vinylpyridine was neutralized by addition of triethanolamine (1.25 M, 6 µL). The 2-vinylpyridine-treated cell extract (20 µL) was assayed for GSSG amount as described above.

The amount of GSH and GSSG was normalized to cellular protein using Bradford assay. The GSH/GSSG ratio was calculated by the following formula:

GSH/GSSG ratio = (Total glutathione – GSSG)/GSSG

VIII. Determination of reactive oxygen species (ROS)

An intracellular ROS level generated from doxorubicin was determined by CellROX® deep red. This reagent is a cell-permeant dye which is non-fluorescent at reduced state, but exhibits strong fluorescent signal upon oxidation by ROS. Briefly, the cells were washed once with DMEM and incubated with 5 µM of CellROX® deep red in DMEM at 37°C for 30 min. Then, cells were washed three times with PBS and trypsinized with trypsin-EDTA solution at 37°C. The cells were pelleted and fixed in 4% formaldehyde in PBS. The intensity of CellROX® deep red fluorescence was measured by BD FACSCalibur flow cytometer at 635 and 661/16 nm for excitation and emission wavelengths, respectively. The fluorescent intensity of 10,000 events was used for data analysis.

Data analysis

Data were expressed as mean ± standard error of the mean (SEM) from at least three independent experiments (n=3). The statistical analysis was performed either by Mann-Whitney *U* test or Kruskal-Wallis test, followed by Mann-Whitney *U* test with Bonferroni correction, where appropriate. Statistical significance was considered at p-value<0.05.

CHAPTER IV
RESULTS

I. Identification of Caco-2 cell differentiation states

The differentiation states of Caco-2 cells were identified based on changing of three differentiation markers including cell numbers, percentage of cells in G_0/G_1 phase, and alkaline phosphatase (ALP) activity during the culture period of 21 days. In this study, the cells reached their confluency at day 3 after seeding. As shown in Figure 1 and 2, the cell numbers and cell population in G_0/G_1 phase increased in time-dependent manner and reached the plateau phase around day 7. The cellular ALP activity was very low when the cells were in proliferative phase (day 1-3) before reaching their confluency. After the cells were confluent (day 3), the ALP activity gradually increased and reached the plateau phase around day 11 after seeding (Figure 3). These findings suggested apparent three growth states of Caco-2 cells which included the pre-, during-, and post-differentiation states (Figure 4) with their characteristics summarized in Table 1.

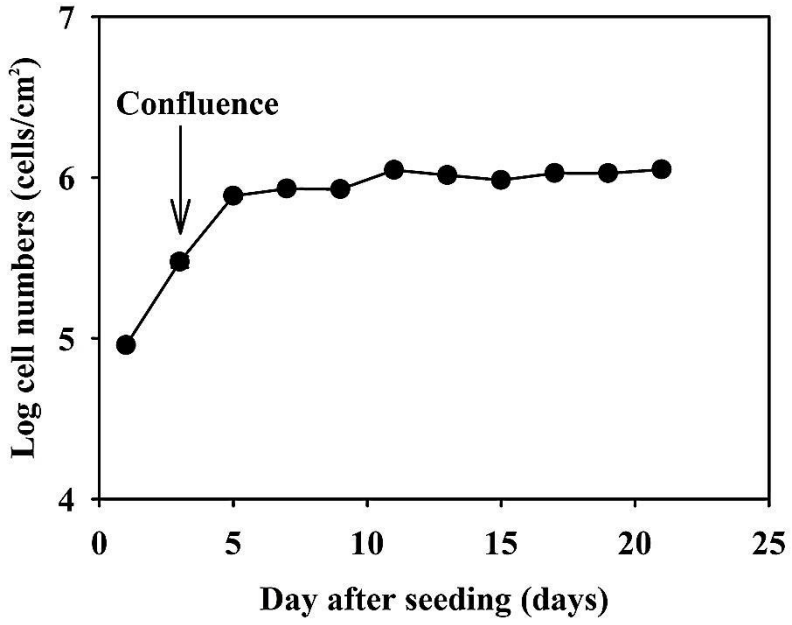

Figure 1: Total cell numbers of Caco-2 cells during 21-day culturing period. Data are expressed as mean ± SEM (n=3, duplicates).

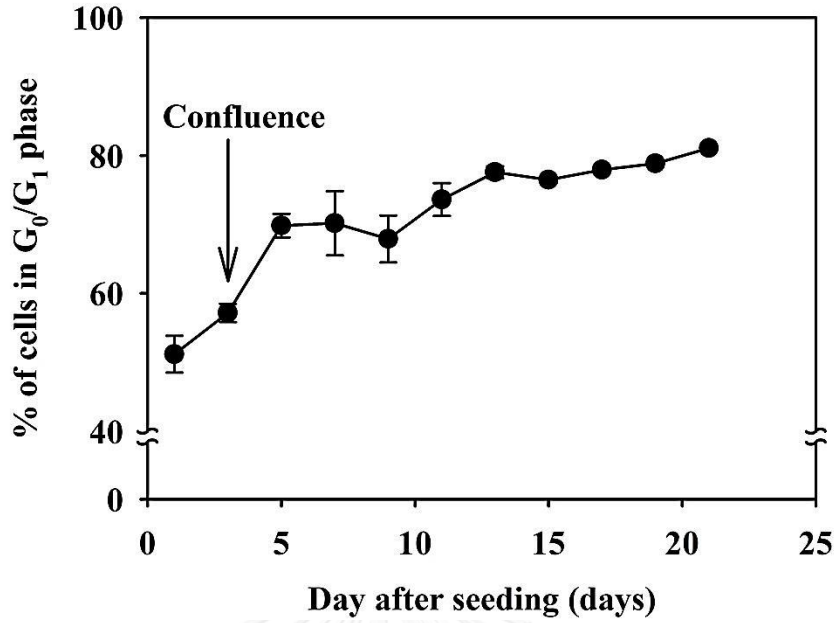

Figure 2: Percentage of Caco-2 cells in G_0/G_1 phase during 21-day culturing period. Data are expressed as mean ± SEM (n=3).

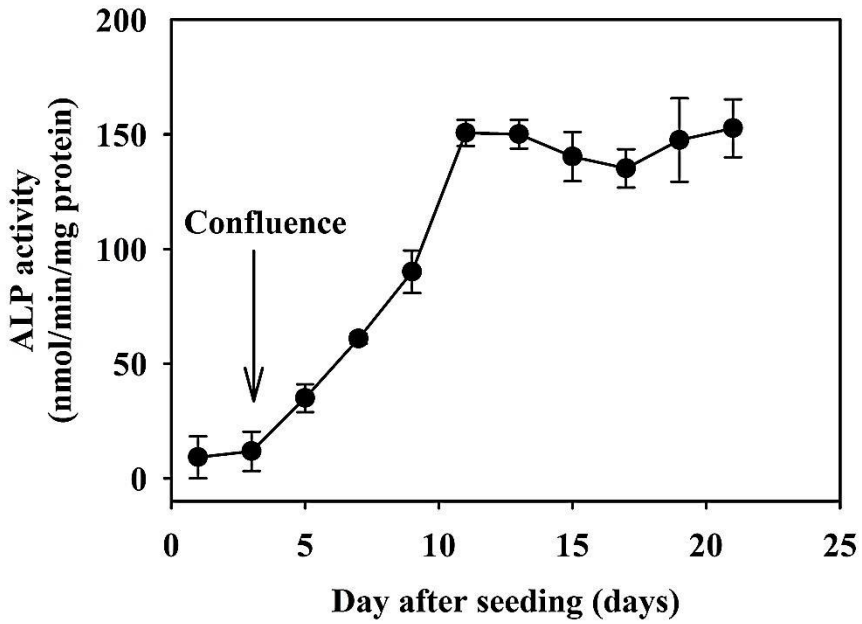

Figure 3 Alkaline phosphatase (ALP) activity of Caco-2 cells during 21-day culturing period. Data are expressed as mean ± SEM (n=3, duplicates).

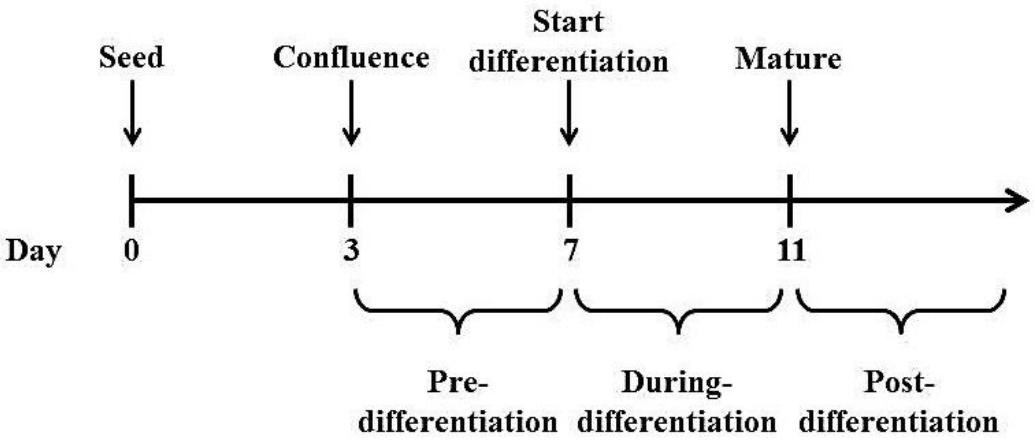

Figure 4: Proposed time course of Caco-2 differentiation phases.

Table 1: Differentiation profile of Caco-2 cells based on differentiation markers used in this study.

Differentiation markers	Pre-differentiation	During-differentiation	Post-differentiation
Confluency	Confluence	Confluence	Confluence
Growth curve	Log phase	Plateau	Plateau
Phase of cell cycle	No arrest	G_0/G_1 arrest	G_0/G_1 arrest
ALP activity	Very low	Rising phase	Plateau

In addition, the extent of *ABCB1* mRNA and P-gp level expressed at each growth state were determined by RT-qPCR and western blot analysis, respectively. The extent of *ABCB1* mRNA was at the highest level when the cells were in the pre-differentiation state. The cells in the during-differentiation state had the lowest *ABCB1* mRNA level, comparing with the cells in other growth states. Moreover, the extent of *ABCB1* mRNA in the cells at the pre- and post-differentiation states was comparable (Figure 5). In contrast, the P-gp protein was expressed at the highest level in the pre-differentiated cells. The amount of P-gp protein markedly decreased as the cells were further grown into differentiation phase (Figure 6).

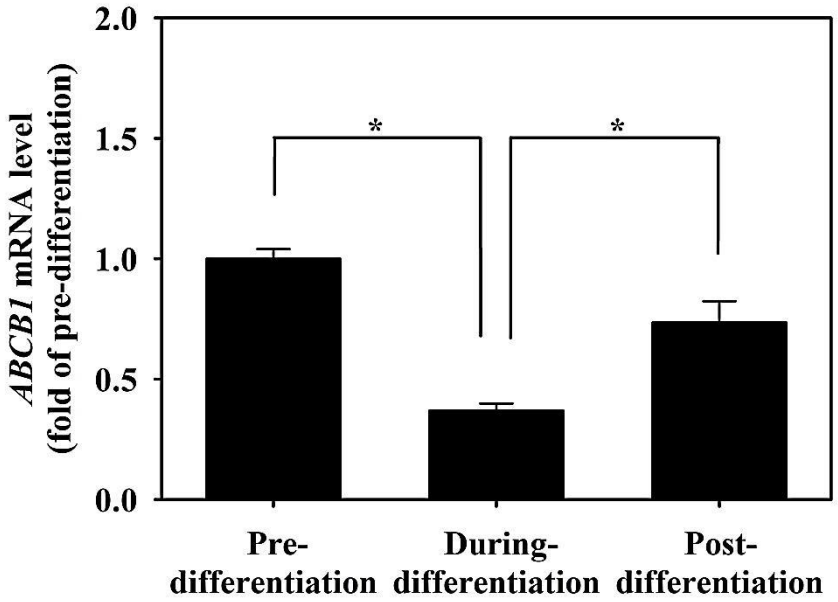

Figure 5: Basal expression level of *ABCB1* mRNA in the Caco-2 cells at different growth states in relative to those expressed in the pre-differentiation state. Data are expressed as mean ± SEM (n=3, triplicates). **p*<0.05 indicated statistical significance.

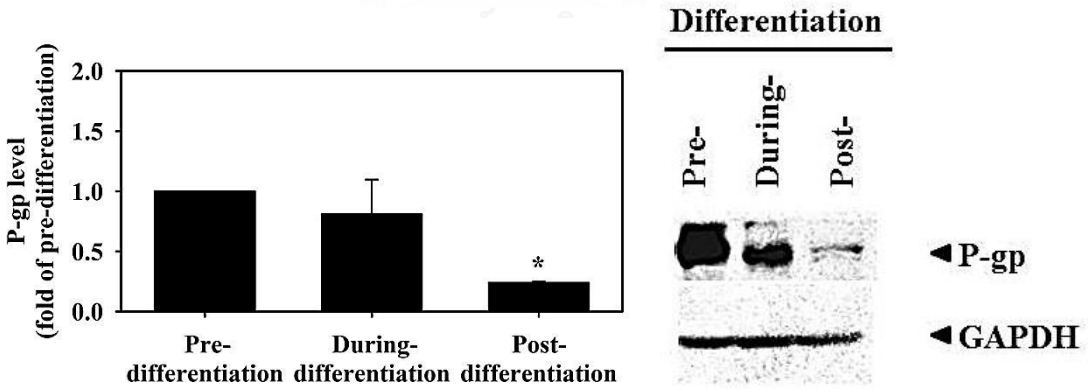

Figure 6: Western blot analysis of P-gp expression in Caco-2 cells at different growth states. Data are expressed as mean ± SEM (n=3). **p*<0.05 indicated statistical significance from the pre-differentiated cells.

II. Effect of doxorubicin on *ABCB1*/P-gp expression in each differentiation state of Caco-2 cells

At 24-hour treatment, doxorubicin at the concentrations up to 100 μM had no effect on the cell viability of Caco-2 cells (Figure 7). The survival rates of the cells in each growth state were greater than 80%. In addition, doxorubicin had no effect on cellular ALP activity of Caco-2 cells in each growth state (Figure 8).

As shown in Figure 9, an alteration of *ABCB1* mRNA level in Caco-2 cells was not in linear relationship with the concentrations of doxorubicin. In the pre- and post-differentiated Caco-2 cells, doxorubicin at the concentrations up to 10 μM caused a significant increase of *ABCB1* mRNA. However, doxorubicin at the high concentrations (50 and 100 μM) did not affect *ABCB1* mRNA level in these cells. The biphasic responses toward doxorubicin treatment were observed in the during-differentiated Caco-2 cells. Doxorubicin up to 5 μM was able to increase *ABCB1* mRNA level in these cells. However, the extent of *ABCB1* mRNA decreased in the cells treated with doxorubicin at the concentration of greater than 10 μM. At the concentration of 100 μM, doxorubicin downregulated the *ABCB1* mRNA level significantly.

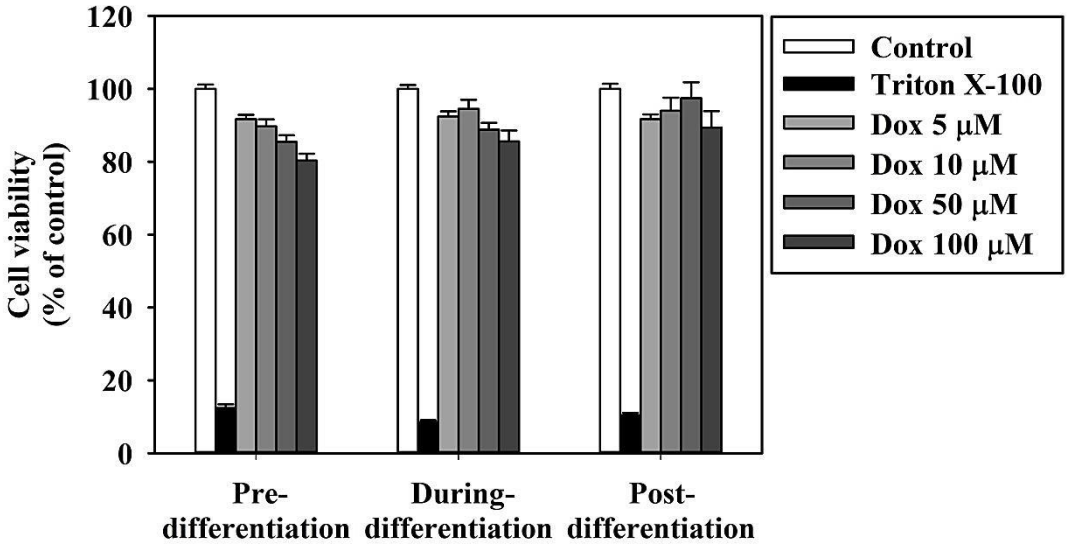

Figure 7: Effect of doxorubicin (Dox) on cell viability of Caco-2 cells. Triton X-100 (0.1%) was used as a positive control. Data are expressed as mean ± SEM (n=3, duplicates).

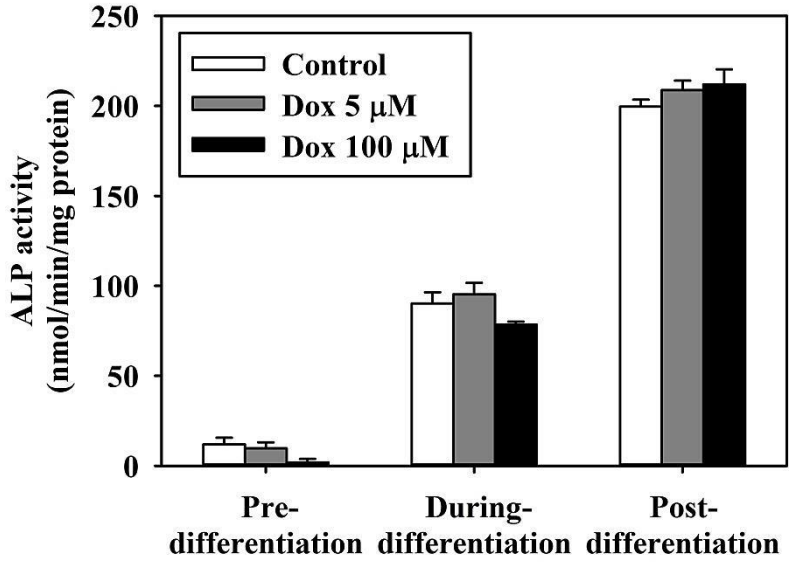

Figure 8 Effect of doxorubicin (Dox) on ALP activity in each differentiation state of Caco-2 cells. Data are expressed as mean ± SEM (n=3, duplicates).

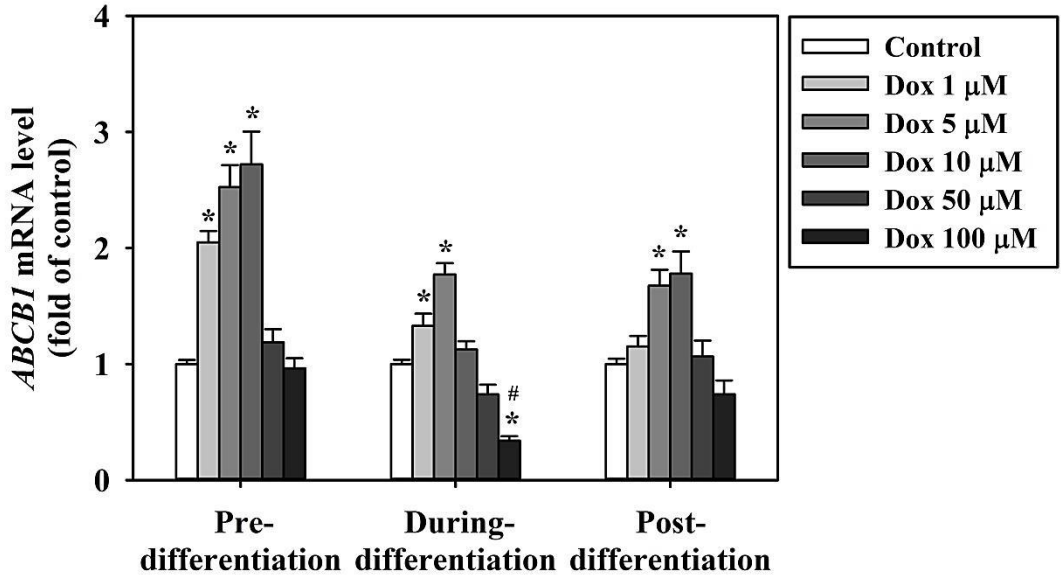

Figure 9: Effect of doxorubicin (Dox) on *ABCB1* mRNA level in each differentiation state of Caco-2 cells. Data are expressed as mean ± SEM (n=3-6, triplicates). *p<0.05 indicated statistical significance from the control group. $^{\#}p$<0.05 indicated statistical significance from the doxorubicin 5 μM.

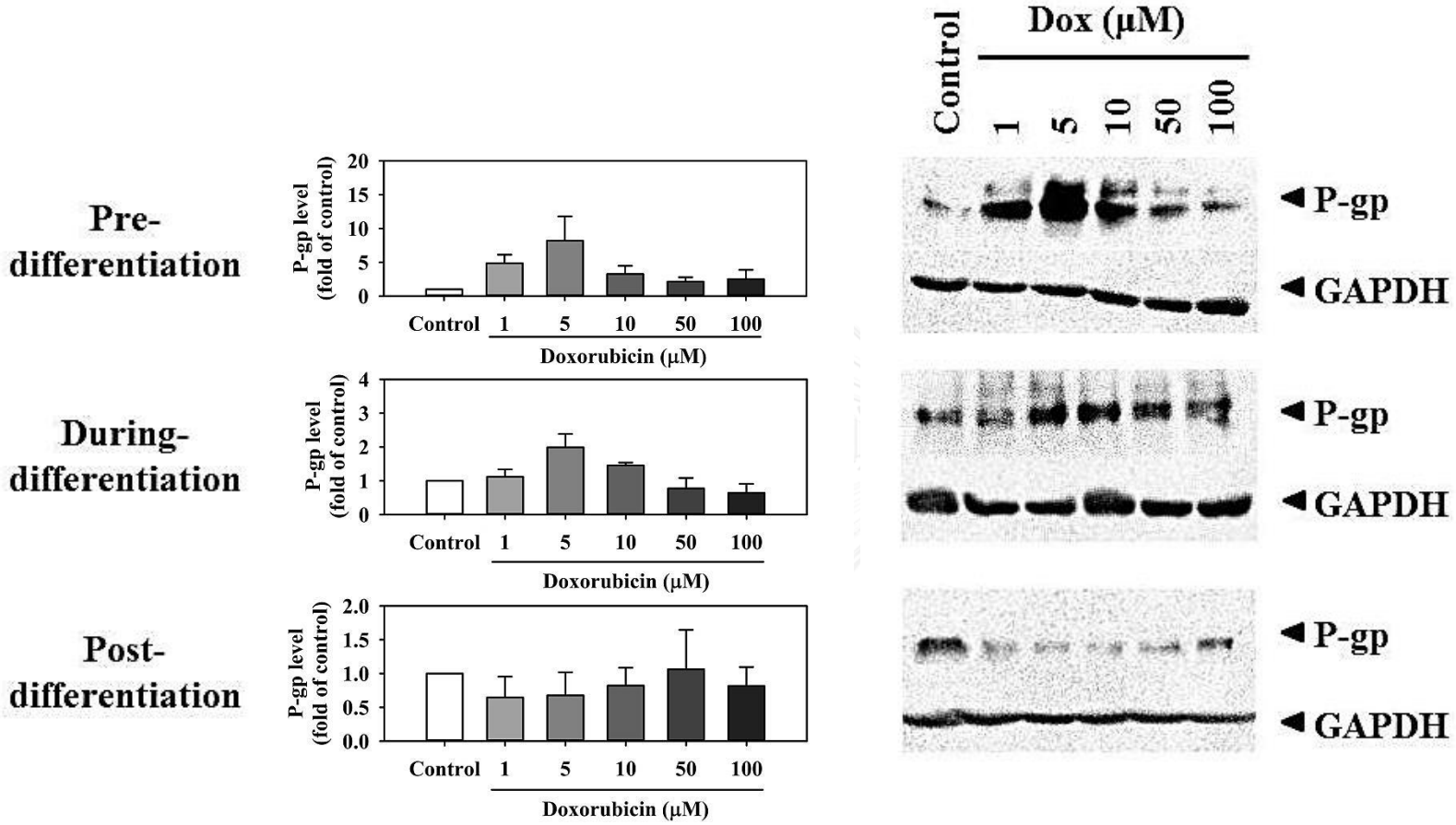

Figure 10: Effect of doxorubicin (Dox) on P-gp expression in each differentiation state of Caco-2 cells. The amount of protein loaded onto SDS-PAGE was 20 μg per lane with an exception of 30 μg per lane when the protein was extracted from the post-differentiated cells. Data are expressed as mean ± SEM (n=3).

In addition, the expression profiles of *ABCB1* protein (P-gp) obtained from doxorubicin-treated Caco-2 cells at the pre- and during-differentiation states were corresponded to their mRNA levels. At the concentrations up 10 μM, doxorubicin increased the expression of P-gp protein level. Interestingly, alteration of *ABCB1* mRNA and P-gp levels in the post-differentiated Caco-2 cells treated with doxorubicin were not correlated. Apparently, doxorubicin (up to 100 μM) suppressed P-gp protein expression (Figure 10).

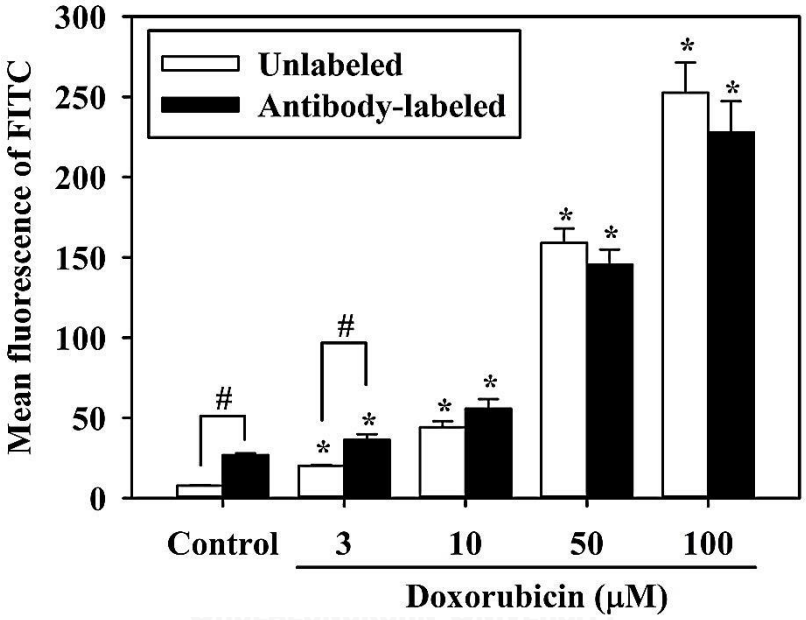

Figure 11: An interfering effect of doxorubicin on fluorescent intensity of the fluorescein isothiocyanate (FITC)-conjugated antibody-labeled and the unlabeled cells. Data are expressed as mean ± SEM (n=3, duplicates). *p<0.05 indicated statistical significance from the control group. $^{\#}p$<0.05 indicated statistical significance between the antibody-labeled and the unlabeled groups.

Furthermore, the effect of doxorubicin on expression of P-gp on the cell surface was determined using fluorescein isothiocyanate (FITC)-conjugated anti-P-gp antibody. However, the preliminary data suggested that flow cytometric measurement of surface P-gp could not be determined due to an interfering effect of doxorubicin. As shown in Figure 11, the cells in the control group which were antibody-labeled

showed a significant increase in fluorescent intensity, suggesting the presence of considerable amount of expressed P-gp in these cells. In the cells treated with 3 μM of doxorubicin, the intensity of the fluorescence between antibody-labeled and unlabeled cells was statistically different. Upon increasing the concentration of doxorubicin, fluorescent signals of the antibody-labeled cells were apparently equal to those of the unlabeled cells (Figures 11). This data clearly demonstrated that doxorubicin, particularly at concentrations higher than 3 μM, was able to interfere with the fluorescent signal of FITC-conjugated antibody on the cell surface.

III. An involvement of cellular redox status and reactive oxygen species (ROS) in doxorubicin-mediated *ABCB1* upregulation

Cellular redox status was identified based on the ratio of reduced glutathione (GSH) and oxidized glutathione (GSSG). The amount of GSH and GSSG was quite comparable in the cells at three growth states (Figure 12A). In addition, the GSH/GSSG ratio apparently shifted to the more reduced state when the cells underwent differentiation (Figure 12B).

An intracellular ROS level generated by doxorubicin was determined in Caco-2 cells at each differentiation state. As shown in Figure 13, doxorubicin at the concentration of 5 μM significantly increased an intracellular ROS level in the pre-differentiated cells, as compared to the control group. In contrast, doxorubicin had no such effect in Caco-2 cells in the during- and post-differentiation states. The presence of *N*-acetylcysteine (NAC) significantly inhibited an increase of intracellular ROS caused by doxorubicin in the pre-differentiated cells, when compared to doxorubicin alone (Figure 14). These data suggested that doxorubicin could generate intracellular ROS in Caco-2 cells at the pre-, but not at the during- and post-differentiation states.

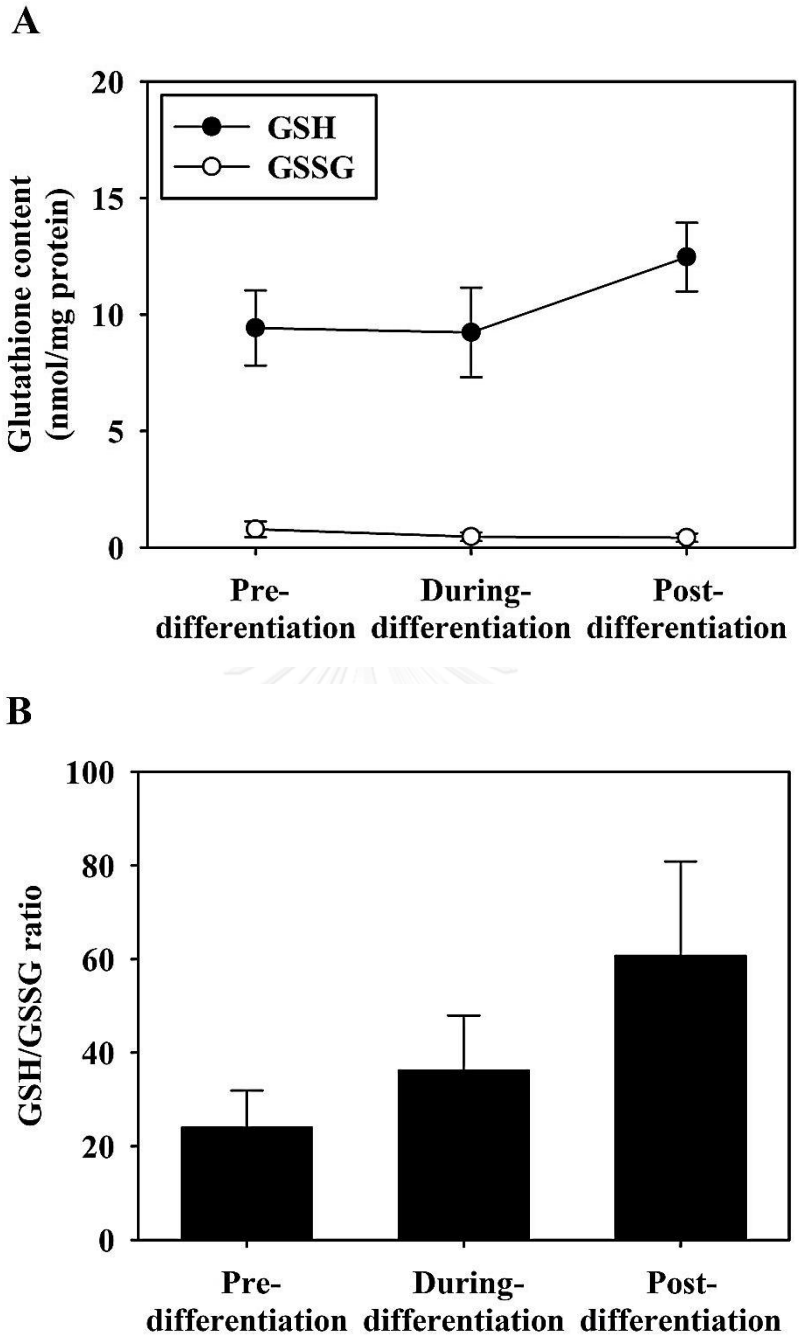

Figure 12: Glutathione at each differentiation state of Caco-2 cells. A) The amount of glutathione in reduced form (GSH) and oxidized form (GSSG). B) The GSH/GSSG ratio. Data are expressed as mean ± SEM (n=5).

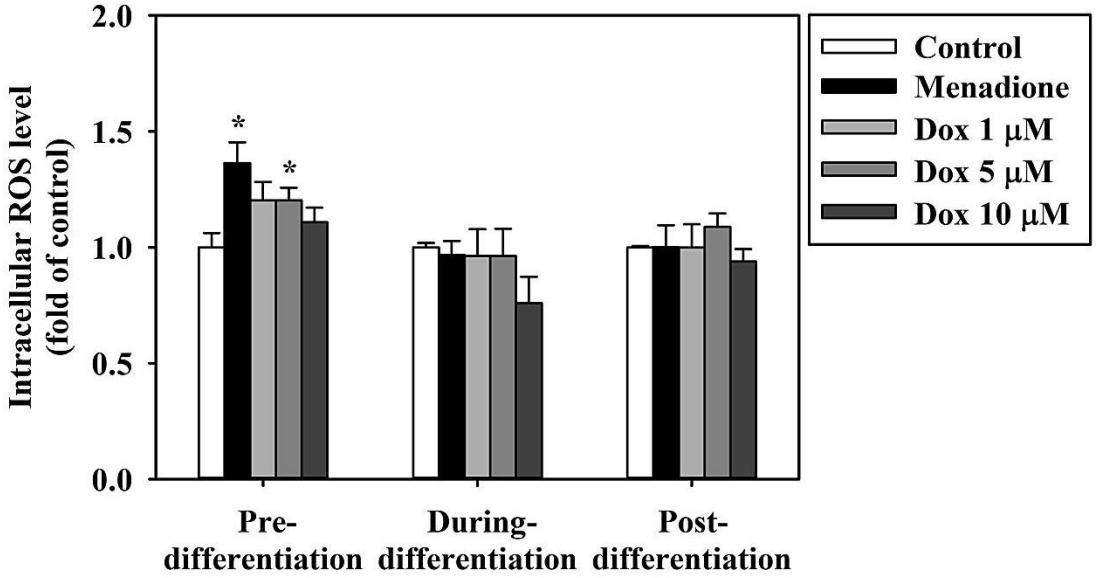

Figure 13: Effect of doxorubicin (Dox) on intracellular ROS level in each differentiation state of Caco-2 cells. Menadione (10 μM) was used as a positive control. Data are expressed as mean ± SEM (n=3-6, duplicates). *p<0.05 indicated statistical significance from the control group.

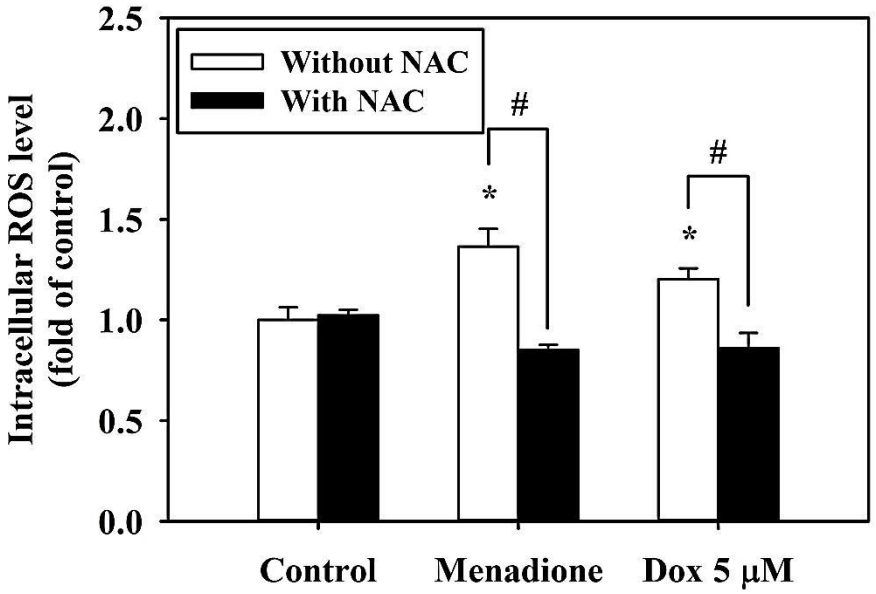

Figure 14: Effect of doxorubicin (Dox) with and without *N*-acetylcysteine (NAC) on intracellular ROS level in the pre-differentiated Caco-2 cells. Menadione (10 μM) was used as a positive control. Data are expressed as mean ± SEM (n=3-6, duplicates). *p<0.05 indicated statistical significance from the control group. $^{\#}p$<0.05 indicated statistical significance between with NAC and without NAC groups.

An involvement of ROS in the doxorubicin-mediated *ABCB1* alteration was determined in Caco-2 cells at each growth state. As shown in Figure 15 and 16, NAC significantly inhibited an increase of *ABCB1* mRNA level induced by doxorubicin (5 μM) in the pre- and during-differentiated cells. On contrary, NAC had no effect on doxorubicin-mediated upregulation in the post-differentiated cells (Figure 17). Interestingly, NAC was able to increased *ABCB1* mRNA level in the pre- and post-differentiated cells (Figure 15 and 17). Moreover, NAC could not entirely prevent the downregulation of *ABCB1* mRNA caused by doxorubicin 100 μM in the during-differentiated cells (Figure 16). These data suggested that ROS might take part in a mechanism of doxorubicin-mediated *ABCB1* alteration. In addition, the growth states of Caco-2 cells could affect cellular response toward doxorubicin treatment at transcription level.

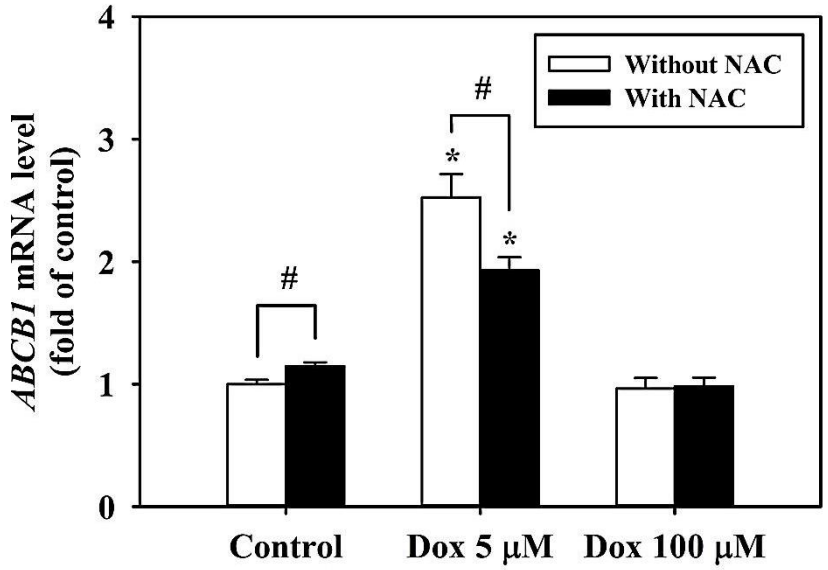

Figure 15: Effect of doxorubicin (Dox) with and without *N*-acetylcysteine (NAC) on *ABCB1* mRNA level in the pre-differentiated Caco-2 cells. Data are expressed as mean ± SEM (n=3-6, triplicates). *$p<0.05$ indicated statistical significance from the control group. $^{\#}p<0.05$ indicated statistical significance between with NAC and without NAC groups.

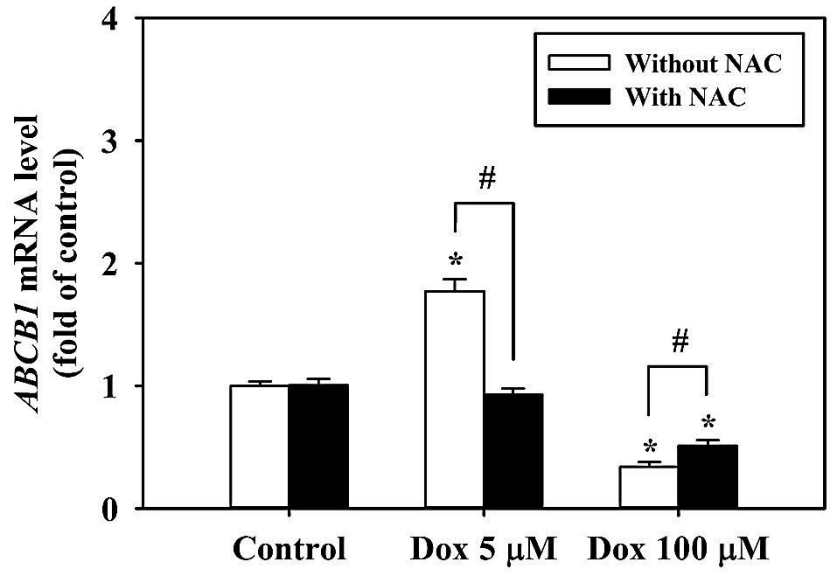

Figure 16: Effect of doxorubicin (Dox) with and without *N*-acetylcysteine (NAC) on *ABCB1* mRNA level in the during-differentiated Caco-2 cells. Data are expressed as mean ± SEM (n=3-6, triplicates). **p*<0.05 indicated statistical significance from the control group. $^{\#}p$<0.05 indicated statistical significance between with NAC and without NAC groups.

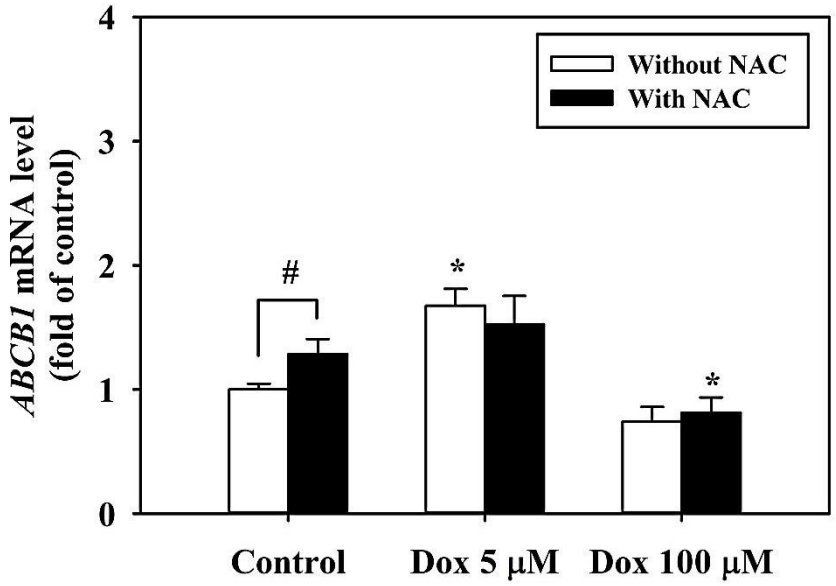

Figure 17: Effect of doxorubicin (Dox) with and without *N*-acetylcysteine (NAC) on *ABCB1* mRNA level in the post-differentiated Caco-2 cells. Data are expressed as mean ± SEM (n=3-6, triplicates). **p*<0.05 indicated statistical significance from the control group. $^{\#}p$<0.05 indicated statistical significance between with NAC and without NAC groups.

IV. Establishment of sodium butyrate-induced cell differentiation model

Doxorubicin-mediated alteration of *ABCB1* mRNA was also determined in an accelerated differentiation model of Caco-2. In this study, the differentiation of Caco-2 cells was accelerated through addition of sodium butyrate (NaBT). The cells in each differentiation phase were identified based on ALP activity, total cell numbers, and percentage of cells in sub G_0 phase of cell cycle, as describe in materials and methods. As shown in Figure 18, treatment the cells with NaBT up to the concentrations of 10 mM significantly increased ALP activity. At the concentration of 5 mM, NaBT apparently elicited its maximal effect on ALP activity. Increasing NaBT exposure time from 1 to 2 days produced the greater NaBT effect (5 mM; 13.22 folds) on ALP activity (Figure 18). In addition, NaBT was able to slow the proliferation rate and increase the percentage of cells in sub G_0 phase in concentration- and time-dependent manner (Figure 19 and 20). The total cell numbers were correlated with the percentage of cells in sub G_0 phase (apoptotic cells), suggesting that slowed proliferation rate might result from NaBT-mediated apoptosis. In this regard, an accelerated differentiation model of Caco-2 was conducted by treatment the cells with 2 mM NaBT for 2 days (Figure 21). Under this condition, NaBT had the lowest apoptotic effect with an appreciable high ALP activity.

The extent of *ABCB1* mRNA and P-gp level in the NaBT-induced differentiated cells were determined in comparison with those of the pre-differentiated cells. As shown in Figure 22, the extent of *ABCB1* mRNA in the pre-differentiated cells and the NaBT-induced differentiated cells were comparable. In contrast, the extent of P-gp protein was higher in the NaBT-induced differentiated cells than in the pre-differentiated cells (Figure 23).

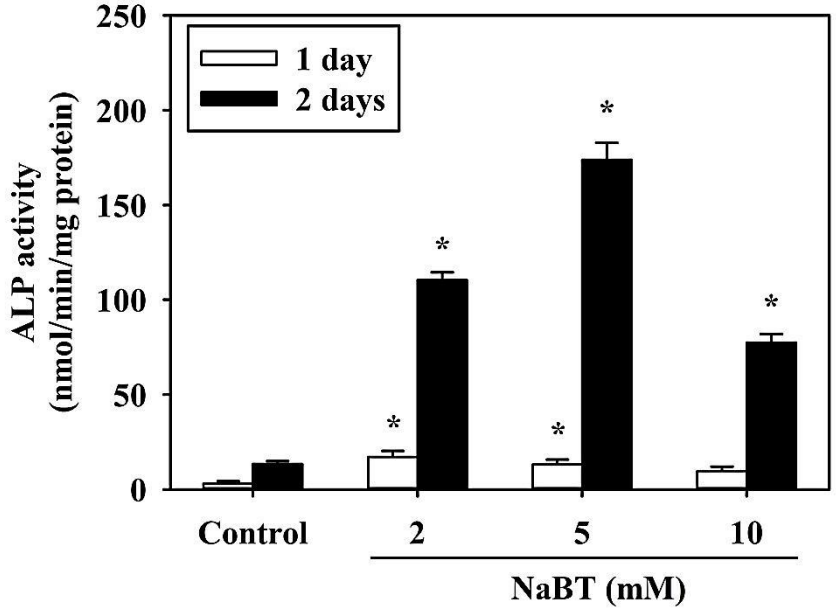

Figure 18: Effect of sodium butyrate (NaBT) on ALP activity. Data are expressed as mean ± SEM (n=3, triplicates). *p<0.05 indicated statistical significance from the control group.

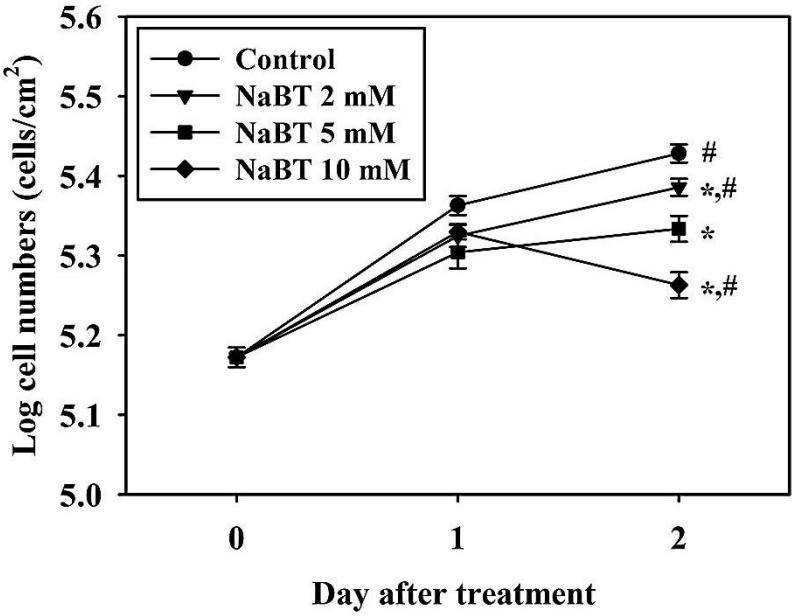

Figure 19: Effect of sodium butyrate (NaBT) on total cell numbers. Data are expressed as mean ± SEM (n=3, triplicates). *p<0.05 indicated statistical significance from the control group. $^{\#}p$<0.05 indicated statistical significance between 1- and 2-day treatment.

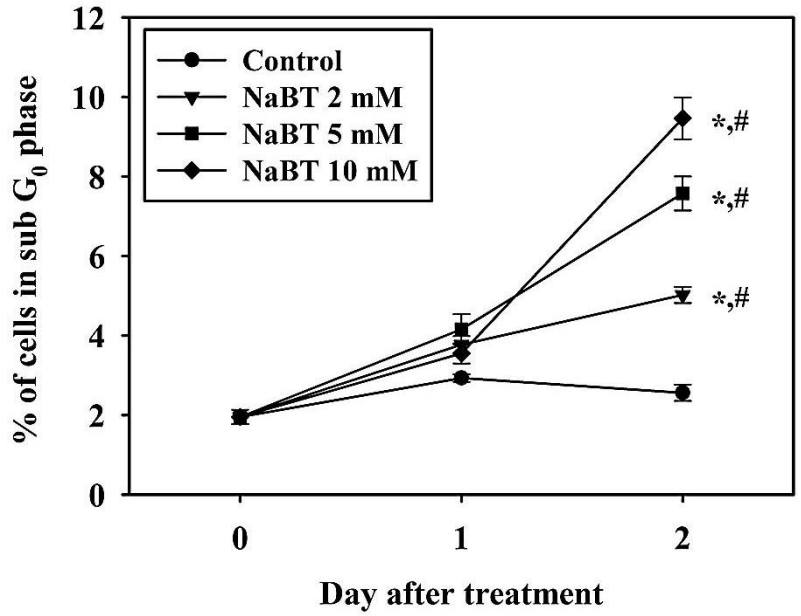

Figure 20: Effect of sodium butyrate (NaBT) on the percentage of cells in sub G_0 phase. Data are expressed as mean ± SEM (n=3). *p<0.05 indicated statistical significance from the control group. #p<0.05 indicated statistical significance between 1- and 2-day treatment.

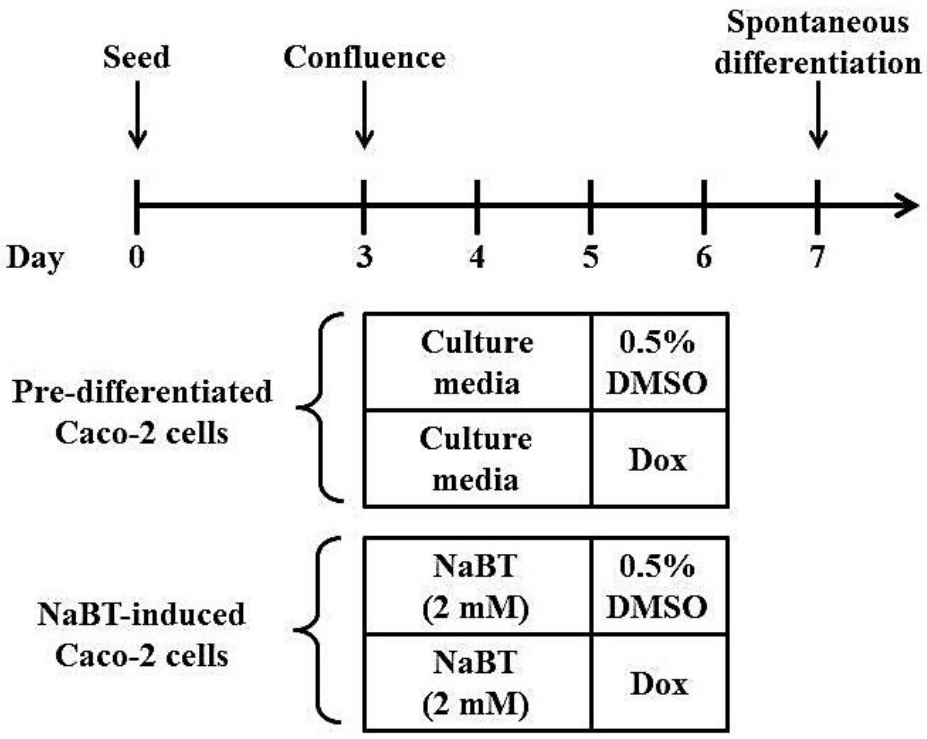

Figure 21: Proposed timeline for NaBT-induced differentiation in Caco-2 cells.

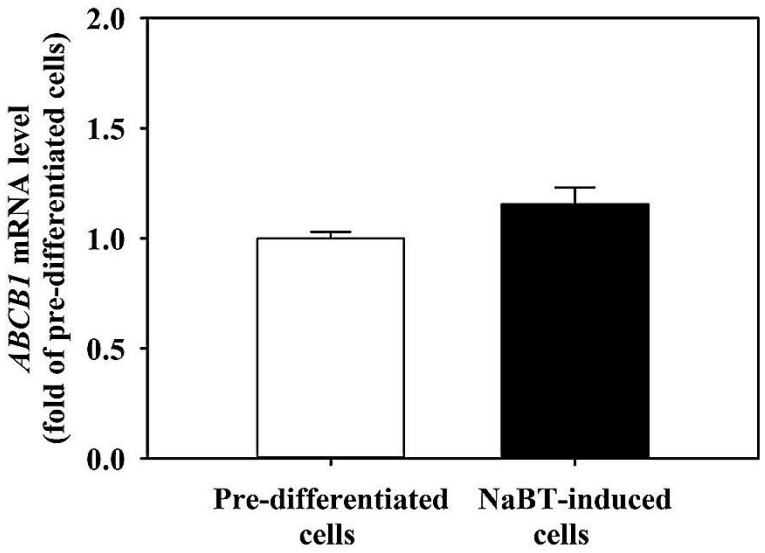

Figure 22: The basal expression of *ABCB1* mRNA in the pre-differentiated and the NaBT-induced differentiated Caco-2 cells. The amount of mRNA was calculated in relative to those in the pre-differentiated cells. Data are expressed as mean ± SEM (n=3, triplicates).

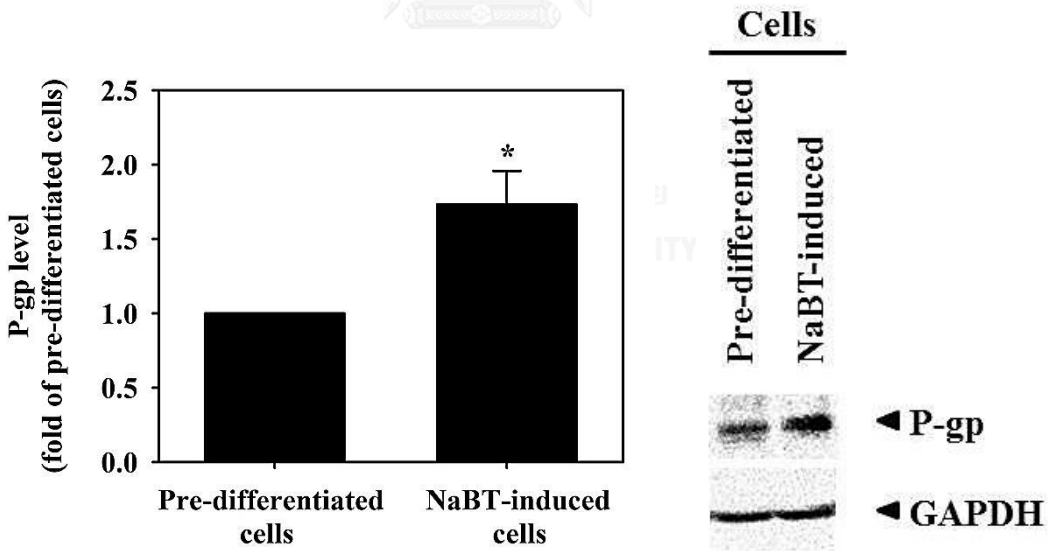

Figure 23: Western blot analysis of P-gp expression in the pre-differentiated and the NaBT-induced differentiated Caco-2 cells. Data are expressed as mean ± SEM (n=3). **p*<0.05 indicated statistical significance from the pre-differentiated cells.

V. Effect of doxorubicin on *ABCB1*/P-gp expression in sodium butyrate-induced cell differentiation model

As shown in Figure 24, the NaBT-induced differentiated cells were more sensitive to doxorubicin cytotoxicity than the pre-differentiated cells. In the NaBT-induced differentiated cells, the non-cytotoxic concentrations of doxorubicin were up to 10 μM at the 24-hour treatment period (Figure 24).

As shown in Figure 25, doxorubicin (5 μM) caused a significant increase of *ABCB1* mRNA level in the pre-differentiated and the NaBT-induced differentiated cells at the comparable degree. However, an effect of doxorubicin on the expressed protein level in these two cell models was otherwise. The extent of P-gp protein in the doxorubicin-treated pre-differentiated cells was corresponded to their mRNA level. In contrast, doxorubicin had no effect on the expression of P-gp protein after 24-treatment in the NaBT-induced differentiated cells (Figure 26).

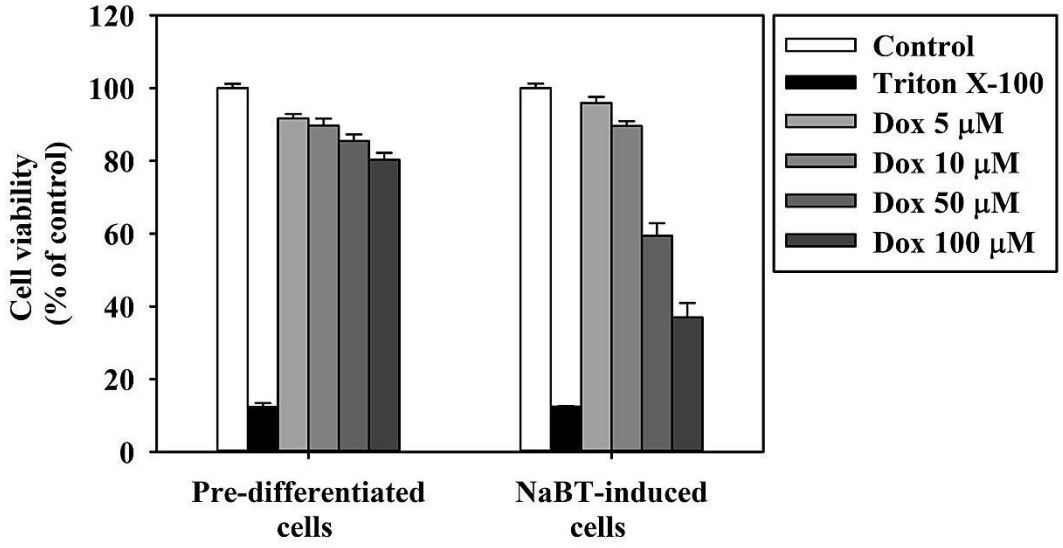

Figure 24: Effect of 24-hour treatment with doxorubicin (Dox) on cell viability of the pre-differentiated and the NaBT-induced differentiated Caco-2 cells. Triton X-100 (0.1%) was used as a positive control. Data are expressed as mean ± SEM (n=3, duplicates).

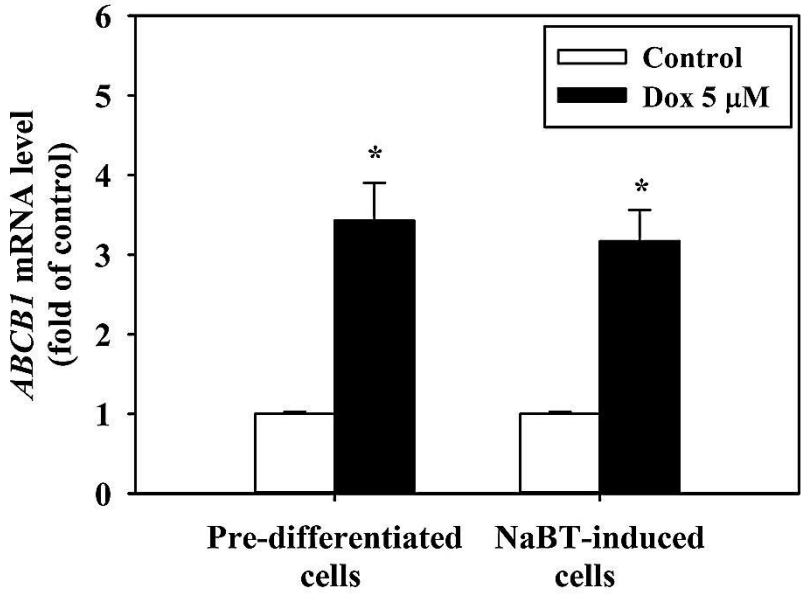

Figure 25: Effect of doxorubicin (Dox) on *ABCB1* mRNA level in the pre-differentiated and the NaBT-induced differentiated Caco-2 cells. Data are expressed as mean ± SEM (n=3, triplicates). **p*<0.05 indicated statistical significance from the control group.

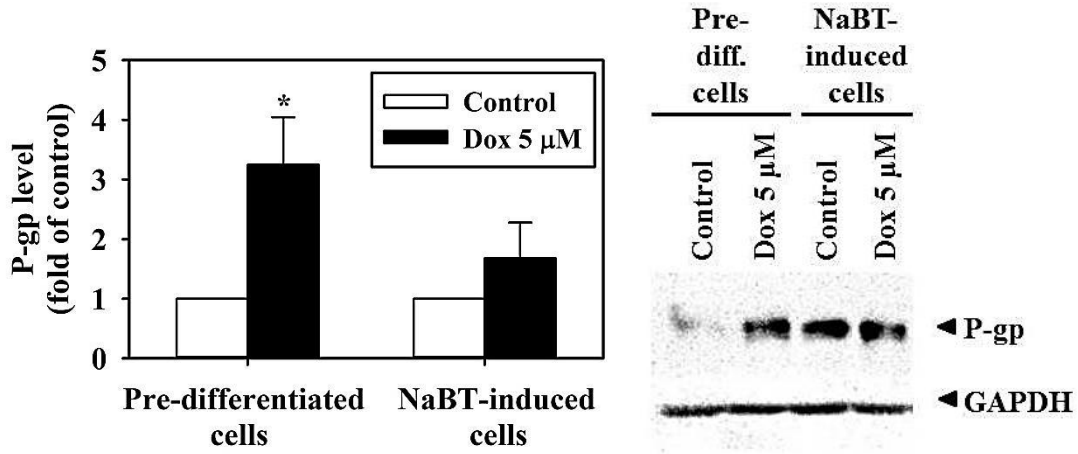

Figure 26: Effect of doxorubicin (Dox) on P-gp expression in the pre-differentiated and the NaBT-induced differentiated cells. Data are expressed as mean ± SEM (n=3). **p*<0.05 indicated statistical significance from the control group.

CHAPTER V
DISCUSSION AND CONCLUSIONS

The differentiation of Caco-2 is the multi-step process which propels the cell transition from colonic to enterocytic cells (Engle et al., 1998). The timeline of Caco-2 differentiation depends on several factors including seeding density, passage numbers, culturing condition, media compositions, and material of cell culture surface (Piana et al., 2008a, Sambuy et al., 2005, Natoli et al., 2012). In this study, the differentiation states of Caco-2 cells were divided into three phases including the pre-, during-, and post-differentiation. The proposed timeline of differentiation, as illustrated in Figure 4, was based on three differentiation markers including cell numbers, percentage of cells in G_0/G_1 phase, and ALP activity. The estimation of growth states could vary among studies due to the applied differentiation markers and decision criteria. In this study, the decision criteria of each differentiation marker were based on their plateau behaviors. As summarized in Table 1, the cells were in the post-differentiation state when all three differentiation markers reached their plateau (day 11). The proliferative cells were considered to be in the pre-differentiation state, which start from reaching confluency to a rising of ALP activity (day 3 to 6). The cells in between the pre- and the post-differentiation states were defined as the during-differentiated cells (day 7 to 10).

The expression of efflux drug transporters in particular P-gp depended on the differentiation status of Caco-2 cells (Kamiyama et al., 2009, Goto et al., 2003). In this study, the extent of both *ABCB1* mRNA and P-gp decreased when cells were further grown into differentiation phase. These finding were in agreement with other reports that *ABCB1* mRNA and P-gp expressed at the highest level in the pre-confluent Caco-2 cells (Goto et al., 2003). This might be due to a more stability and higher transcription rate of *ABCB1* mRNA of the cells in this growth state. The expression level of *ABCB1* mRNA and P-gp decreased when the cells shifted from the proliferation to the differentiation phase (Goto et al., 2003). Recently, a strong correlation between basal *ABCB1* mRNA and P-gp expression was demonstrated in wild-type and vinblastine-resistant Caco-2 cells in the confluent state (Shirasaka et al.,

2009). In this study, the basal expression level of *ABCB1* mRNA was correlated to P-gp protein level in the pre- and the during-differentiated cells. However, the correlation between *ABCB1* mRNA and its protein was not observed in the post-differentiated cells.

Doxorubicin could affect *ABCB1*/P-gp expression at transcription level in Caco-2 cells at all growth states. However, an effect of doxorubicin on *ABCB1* mRNA level in Caco-2 cells was not in linear relationship with its concentrations. In the pre- and post-differentiated cells, *ABCB1* mRNA level increased upon treatment with doxorubicin at low concentrations (up to 10 μM). At the high concentrations (50 and 100 μM), doxorubicin had no effect on transcription process of *ABCB1* gene. Exclusively, doxorubicin (100 μM) could suppress *ABCB1* mRNA level significantly in the Caco-2 cells at the during-differentiation phase. As known, doxorubicin potently inhibits several macromolecule biosynthesis (Gewirtz, 1999). At the transcription level, doxorubicin was demonstrated to produce a dramatic conformational distortion at location embracing promoter, leading to transcriptional inhibition of human *c-myc, c-fos, and hsp70* genes (Collins et al., 2001). It was possible that doxorubicin at the high concentrations inhibited the transcription of *ABCB1* mRNA. Nevertheless, the mechanisms underlying doxorubicin-mediated *ABCB1* downregulation in the during-differentiated cells remained to be clarified. In addition to *ABCB1* mRNA, the P-gp profiles in the pre- and the during-differentiated Caco-2 cells were in the same pattern as their mRNA profiles. Interestingly, the effect of doxorubicin at the concentration of 100 μM in the pre-differentiated cells disagreed with those reported. It was reported that doxorubicin (100 μM) caused a 7-fold increase of P-gp level as measured by flow cytometry in the confluent pre-differentiated Caco-2 cells (Silva et al., 2011). This contradictory result might be due to an interference of doxorubicin, in particular at high concentrations, on FITC-labeled anti-P-gp antibody in flow cytometric measurement. The results in this study demonstrated that there was no difference between antibody-labeled and unlabeled cells treated with doxorubicin. It was likely that an increase of fluorescent intensity in flow cytometry resulted from intrinsic fluorescence of doxorubicin rather than an overexpression of P-gp. Taken together, these findings suggested that

doxorubicin at the high concentrations (50 and 100 μM) had no effect on P-gp level in the pre-differentiated Caco-2 cells.

Doxorubicin could interfere with *ABCB1*/P-gp expression through several mechanisms, including ROS-mediated mechanisms (Chen et al., 2012, Komori et al., 2014, Ohkawa et al., 1994). It was reported that cellular redox status of Caco-2 cells shifted toward a more oxidized state, as indicated by a decrease in GSH/GSSG ratio (Nkabyo et al., 2002). Hence, the differentiated cells might be more sensitive to doxorubicin-mediated alteration of P-gp expression than the cells in other growth states. In this study, the GSH/GSSG ratio apparently shifted to a more reduced state when the cells differentiated. Apparently, the cellular redox status was correlated with doxorubicin-generating intracellular ROS. The results demonstrated that doxorubicin (5 μM) significantly increased intracellular ROS level only in the pre-differentiated cells, but not in the during- or the post-differentiated cells. Therefore, it was likely that the apparent oxidized state of the pre-differentiated cells might favorably enable doxorubicin to generate more ROS than other growth phases. As known, *N*-acetylcysteine (NAC) is a universal antioxidant which potentially quenches ROS by direct chemical reaction and being a substrate for glutathione biosynthesis (Kerksick and Willoughby, 2005). In the pre-differentiated cells, NAC was able to entirely inhibit ROS production, and partially inhibited upregulation of *ABCB1* mRNA. In the during-differentiation phase, the *ABCB1* transcription was apparently sensitive toward doxorubicin treatment. Doxorubicin was able to either increase or decrease mRNA levels, depending upon its concentration. In this study, NAC potentially blocked doxorubicin-mediated upregulation of *ABCB1* mRNA, but it had little effect on doxorubicin-mediated downregulation. In the post-differentiation phase, NAC had no effect on doxorubicin-mediated *ABCB1* upregulation. Taken together, these data suggested that ROS might take part in the mechanism of doxorubicin-mediated *ABCB1* alteration at the transcription level in the pre- and the during-differentiation phases. In addition, ROS might not be involved with doxorubicin-mediated alteration of *ABCB1* mRNA in the post-differentiation state.

In addition to spontaneous differentiation, accelerated differentiation of Caco-2 cells could be obtained by treatment the cells with certain substances such as short-chain fatty acids, materials of cell culture surface, and specific types of culture

media (Deng et al., 2013, Malago et al., 2003, Sevin et al., 2013). In this study, the differentiation of Caco-2 cells was accelerated through addition of sodium butyrate (NaBT). NaBT could induce cell differentiation in simultaneous with apoptosis in Caco-2 cells (Ruemmele et al., 2003, Mariadason et al., 2001). Hence, the decision criteria for the NaBT-induced differentiated cells were based on three differentiation markers including cell numbers, percentage of cells in sub G_0 phase, and ALP activity in order to obtain the cells with the maximal differentiation state and the least apoptosis. As illustrated in Figure 21, treatment the cells with 2 mM NaBT for 2 day was a suitable model of accelerated differentiation in this study. The NaBT-treated cells had a comparable *ABCB1* mRNA level with slightly higher P-gp level comparing to those of the pre-differentiated cells (Cummins et al., 2001).

Doxorubicin (5 μM) could upregulate *ABCB1* mRNA level in the NaBT-induced differentiated cells at the similar degree to that of the pre-differentiated cells. In contrast, doxorubicin had no effect on P-gp level in NaBT-induced differentiated cells. These results suggested that the protein expression of *ABCB1* gene in response to doxorubicin treatment was affected by NaBT. Consequently, the NaBT-induced differentiated cells were resistant to an upregulation of P-gp level induced by 5 μM doxorubicin.

In conclusion, this study demonstrated for the first time that the differentiation state of Caco-2 cells strongly affects doxorubicin-mediated *ABCB1*/P-gp expression. The cellular redox status was correlated to an intracellular ROS level, but not an alteration of *ABCB1* mRNA level induced by doxorubicin. In addition, the spontaneous differentiation model and the NaBT-accelerated differentiation model exhibited different responses toward doxorubicin effect on *ABCB1*/P-gp expression.

REFERENCES

ABOLHODA, A., WILSON, A. E., ROSS, H., DANENBERG, P. V., BURT, M. & SCOTTO, K. W. 1999. Rapid activation of MDR1 gene expression in human metastatic sarcoma after in vivo exposure to doxorubicin. *Clin Cancer Res,* 5**,** 3352-6.

AGGARWAL, S., SUZUKI, T., TAYLOR, W. L., BHARGAVA, A. & RAO, R. K. 2011. Contrasting effects of ERK on tight junction integrity in differentiated and under-differentiated Caco-2 cell monolayers. *Biochem J,* 433**,** 51-63.

BENARD, O. & BALASUBRAMANIAN, K. A. 1997. Modulation of glutathione level during butyrate-induced differentiation in human colon derived HT-29 cells. *Mol Cell Biochem,* 170**,** 109-14.

BERTRAM, J., PALFNER, K., HIDDEMANN, W. & KNEBA, M. 1996. Increase of P-glycoprotein-mediated drug resistance by hsp 90 beta. *Anticancer Drugs,* 7**,** 838-45.

BLOUIN, J. M., PENOT, G., COLLINET, M., NACFER, M., FOREST, C., LAURENT-PUIG, P., COUMOUL, X., BAROUKI, R., BENELLI, C. & BORTOLI, S. 2011. Butyrate elicits a metabolic switch in human colon cancer cells by targeting the pyruvate dehydrogenase complex. *Int J Cancer,* 128**,** 2591-601.

BOYD, M., HANSEN, M., JENSEN, T. G., PEREARNAU, A., OLSEN, A. K., BRAM, L. L., BAK, M., TOMMERUP, N., OLSEN, J. & TROELSEN, J. T. 2010. Genome-wide analysis of CDX2 binding in intestinal epithelial cells (Caco-2). *J Biol Chem,* 285**,** 25115-25.

BROWN, G. R., HEM, V., KATZ, K. S., OVETSKY, M., WALLIN, C., ERMOLAEVA, O., TOLSTOY, I., TATUSOVA, T., PRUITT, K. D., MAGLOTT, D. R. & MURPHY, T. D. 2015. Gene: a gene-centered information resource at NCBI. *Nucleic Acids Res,* 43**,** D36-42.

BUDDE, T., HANEY, J., BIEN, S., SCHWEBE, M., RIAD, A., TSCHOPE, C., STAUDT, A., JEDLITSCHKY, G., FELIX, S. B., KROEMER, H. K. & GRUBE, M. 2011. Acute exposure to doxorubicin results in increased cardiac P-glycoprotein expression. *J Pharm Sci,* 100**,** 3951-8.

BUSTIN, S. A., BENES, V., GARSON, J. A., HELLEMANS, J., HUGGETT, J., KUBISTA, M., MUELLER, R., NOLAN, T., PFAFFL, M. W., SHIPLEY, G. L., VANDESOMPELE, J. & WITTWER, C. T. 2009. The MIQE guidelines: minimum information for publication of quantitative real-time PCR experiments. *Clin Chem,* 55**,** 611-22.

CHANTRET, I., BARBAT, A., DUSSAULX, E., BRATTAIN, M. G. & ZWEIBAUM, A. 1988. Epithelial polarity, villin expression, and enterocytic differentiation of cultured human colon carcinoma cells: a survey of twenty cell lines. *Cancer Res,* 48**,** 1936-42.

CHEN, Y., ZHAO, Y., WANG, C., XIAO, X., ZHOU, X. & XU, G. 2012. Inhibition of p38 MAPK diminishes doxorubicin-induced drug resistance associated with P-glycoprotein in human leukemia K562 cells. *Med Sci Monit,* 18**,** BR383-8.

COLLINS, I., WEBER, A. & LEVENS, D. 2001. Transcriptional consequences of topoisomerase inhibition. *Mol Cell Biol,* 21**,** 8437-51.

CUMMINS, C. L., MANGRAVITE, L. M. & BENET, L. Z. 2001. Characterizing the expression of CYP3A4 and efflux transporters (P-gp, MRP1, and MRP2) in CYP3A4-transfected Caco-2 cells after induction with sodium butyrate and the phorbol ester 12-O-tetradecanoylphorbol-13-acetate. *Pharm Res,* 18**,** 1102-9.

DENG, X., ZHANG, G., SHEN, C., YIN, J. & MENG, Q. 2013. Hollow fiber culture accelerates differentiation of Caco-2 cells. *Appl Microbiol Biotechnol,* 97**,** 6943-55.

DING, Q. M., KO, T. C. & EVERS, B. M. 1998. Caco-2 intestinal cell differentiation is associated with G1 arrest and suppression of CDK2 and CDK4. *Am J Physiol,* 275**,** C1193-200.

DUAN, R., HU, N., LIU, H. Y., LI, J., GUO, H. F., LIU, C., LIU, L. & LIU, X. D. 2012. Biphasic regulation of P-glycoprotein function and expression by NO donors in Caco-2 cells. *Acta Pharmacol Sin,* 33**,** 767-74.

EHRET, M. J., LEVIN, G. M., NARASIMHAN, M. & RATHINAVELU, A. 2007. Venlafaxine induces P-glycoprotein in human Caco-2 cells. *Hum Psychopharmacol,* 22**,** 49-53.

ENGLE, M. J., GOETZ, G. S. & ALPERS, D. H. 1998. Caco-2 cells express a combination of colonocyte and enterocyte phenotypes. *J Cell Physiol,* 174**,** 362-9.

FARDEL, O., LECUREUR, V., DAVAL, S., CORLU, A. & GUILLOUZO, A. 1997. Up-regulation of P-glycoprotein expression in rat liver cells by acute doxorubicin treatment. *Eur J Biochem,* 246**,** 186-92.

FERRUZZA, S., ROSSI, C., SCARINO, M. L. & SAMBUY, Y. 2012a. A protocol for differentiation of human intestinal Caco-2 cells in asymmetric serum-containing medium. *Toxicol In Vitro,* 26**,** 1252-5.

FERRUZZA, S., ROSSI, C., SCARINO, M. L. & SAMBUY, Y. 2012b. A protocol for in situ enzyme assays to assess the differentiation of human intestinal Caco-2 cells. *Toxicol In Vitro,* 26**,** 1247-51.

FLOHE, L. 2013. The fairytale of the GSSG/GSH redox potential. *Biochim Biophys Acta,* 1830**,** 3139-42.

FU, D. & ARIAS, I. M. 2012. Intracellular trafficking of P-glycoprotein. *Int J Biochem Cell Biol,* 44**,** 461-4.

GASCHOTT, T., WERZ, O., STEINMEYER, A., STEINHILBER, D. & STEIN, J. 2001. Butyrate-induced differentiation of Caco-2 cells is mediated by vitamin D receptor. *Biochem Biophys Res Commun,* 288**,** 690-6.

GEWIRTZ, D. A. 1999. A critical evaluation of the mechanisms of action proposed for the antitumor effects of the anthracycline antibiotics adriamycin and daunorubicin. *Biochem Pharmacol,* 57**,** 727-41.

GORRINI, C., HARRIS, I. S. & MAK, T. W. 2013. Modulation of oxidative stress as an anticancer strategy. *Nat Rev Drug Discov,* 12**,** 931-47.

GOTO, M., MASUDA, S., SAITO, H. & INUI, K. 2003. Decreased expression of P-glycoprotein during differentiation in the human intestinal cell line Caco-2. *Biochem Pharmacol,* 66**,** 163-70.

GUSTAFSON, D. L. & LONG, M. E. 2001. Alterations in P-glycoprotein expression in mouse tissues by doxorubicin: implications for pharmacokinetics in multiple dosing regimens. *Chem Biol Interact,* 138**,** 43-57.

HAN, Y., CHIN TAN, T. M. & LIM, L. Y. 2008. In vitro and in vivo evaluation of the effects of piperine on P-gp function and expression. *Toxicol Appl Pharmacol,* 230**,** 283-9.

HAN, Y., TAN, T. M. & LIM, L. Y. 2006. Effects of capsaicin on P-gp function and expression in Caco-2 cells. *Biochem Pharmacol,* 71**,** 1727-34.

HARTZ, A. M., BAUER, B., BLOCK, M. L., HONG, J. S. & MILLER, D. S. 2008. Diesel exhaust particles induce oxidative stress, proinflammatory signaling, and P-glycoprotein up-regulation at the blood-brain barrier. *FASEB J,* 22**,** 2723-33.

HONG, H., LU, Y., JI, Z. N. & LIU, G. Q. 2006. Up-regulation of P-glycoprotein expression by glutathione depletion-induced oxidative stress in rat brain microvessel endothelial cells. *J Neurochem,* 98**,** 1465-73.

HOU, X.-L., TAKAHASHI, K., TANAKA, K., TOUGOU, K., QIU, F., KOMATSU, K., TAKAHASHI, K. & AZUMA, J. 2008. Curcuma drugs and curcumin regulate the expression and function of P-gp in Caco-2 cells in completely opposite ways. *International Journal of Pharmaceutics,* 358**,** 224-229.

HU, X. F., SLATER, A., WALL, D. M., KANTHARIDIS, P., PARKIN, J. D., COWMAN, A. & ZALCBERG, J. R. 1995. Rapid up-regulation of mdr1 expression by anthracyclines in a classical multidrug-resistant cell line. *Br J Cancer,* 71**,** 931-6.

HUANG, R., MURRY, D. J., KOLWANKAR, D., HALL, S. D. & FOSTER, D. R. 2006. Vincristine transcriptional regulation of efflux drug transporters in carcinoma cell lines. *Biochem Pharmacol,* 71**,** 1695-704.

KAMIYAMA, E., SUGIYAMA, D., NAKAI, D., MIURA, S. & OKAZAKI, O. 2009. Culture period-dependent change of function and expression of ATP-binding cassette transporters in Caco-2 cells. *Drug Metab Dispos,* 37**,** 1956-62.

KATAYAMA, K., KAPOOR, K., OHNUMA, S., PATEL, A., SWAIM, W., AMBUDKAR, I. S. & AMBUDKAR, S. V. 2015. Revealing the fate of cell surface human P-glycoprotein (ABCB1): The lysosomal degradation pathway. *Biochim Biophys Acta,* 1853**,** 2361-70.

KATAYAMA, K., NOGUCHI, K. & SUGIMOTO, Y. 2014. Regulations of P-Glycoprotein/ABCB1/MDR1in Human Cancer Cells. *New Journal of Science,* 2014**,** 1-10.

KERKSICK, C. & WILLOUGHBY, D. 2005. The antioxidant role of glutathione and N-acetyl-cysteine supplements and exercise-induced oxidative stress. *J Int Soc Sports Nutr,* 2**,** 38-44.

KOMORI, Y., ARISAWA, S., TAKAI, M., YOKOYAMA, K., HONDA, M., HAYASHI, K., ISHIGAMI, M., KATANO, Y., GOTO, H., UEYAMA, J., ISHIKAWA, T. & WAKUSAWA, S. 2014. Ursodeoxycholic acid inhibits overexpression of P-glycoprotein induced by doxorubicin in HepG2 cells. *Eur J Pharmacol,* 724**,** 161-7.

KONIG, S. K., HERZOG, M., THEILE, D., ZEMBRUSKI, N., HAEFELI, W. E. & WEISS, J. 2010. Impact of drug transporters on cellular resistance towards saquinavir and darunavir. *J Antimicrob Chemother,* 65**,** 2319-28.

LABIALLE, S., GAYET, L., MARTHINET, E., RIGAL, D. & BAGGETTO, L. G. 2002. Transcriptional regulators of the human multidrug resistance 1 gene: recent views. *Biochem Pharmacol,* 64**,** 943-8.

LEDOUX, S., YANG, R., FRIEDLANDER, G. & LAOUARI, D. 2003. Glucose depletion enhances P-glycoprotein expression in hepatoma cells: role of endoplasmic reticulum stress response. *Cancer Res,* 63**,** 7284-90.

LEONI, B. D., NATOLI, M., NARDELLA, M., BUCCI, B., ZUCCO, F., D'AGNANO, I. & FELSANI, A. 2012. Differentiation of Caco-2 cells requires both transcriptional and post-translational down-regulation of Myc. *Differentiation,* 83**,** 116-27.

LIANG, E., CHESSIC, K. & YAZDANIAN, M. 2000. Evaluation of an accelerated Caco-2 cell permeability model. *J Pharm Sci,* 89**,** 336-45.

LIN, J. H. & YAMAZAKI, M. 2003a. Role of P-Glycoprotein in Pharmacokinetics. *Clinical Pharmacokinetics,* 42**,** 59-98.

LIN, J. H. & YAMAZAKI, M. 2003b. Role of P-glycoprotein in pharmacokinetics: clinical implications. *Clin Pharmacokinet,* 42**,** 59-98.

LIU, Z., DUAN, Z. J., CHANG, J. Y., ZHANG, Z. F., CHU, R., LI, Y. L., DAI, K. H., MO, G. Q. & CHANG, Q. Y. 2014. Sinomenine sensitizes multidrug-resistant colon cancer cells (Caco-2) to doxorubicin by downregulation of MDR-1 expression. *PLoS One,* 9**,** e98560.

MA, X., CAI, Y., HE, D., ZOU, C., ZHANG, P., LO, C. Y., XU, Z., CHAN, F. L., YU, S., CHEN, Y., ZHU, R., LEI, J., JIN, J. & YAO, X. 2012. Transient receptor potential channel TRPC5 is essential for P-glycoprotein induction in drug-resistant cancer cells. *Proc Natl Acad Sci U S A,* 109**,** 16282-7.

MALAGO, J. J., KONINKX, J. F., DOUMA, P. M., DIRKZWAGER, A., VELDMAN, A., HENDRIKS, H. G. & VAN DIJK, J. E. 2003. Differential modulation of enterocyte-like Caco-2 cells after exposure to short-chain fatty acids. *Food Addit Contam,* 20**,** 427-37.

MARIADASON, J. M., VELCICH, A., WILSON, A. J., AUGENLICHT, L. H. & GIBSON, P. R. 2001. Resistance to butyrate-induced cell differentiation and apoptosis during spontaneous Caco-2 cell differentiation. *Gastroenterology,* 120**,** 889-99.

MISHRA, J., ZHANG, Q., ROSSON, J. L., MORAN, J., DOPP, J. M. & NEUDECK, B. L. 2008. Lipopolysaccharide increases cell surface P-glycoprotein that exhibits diminished activity in intestinal epithelial cells. *Drug Metab Dispos,* 36**,** 2145-9.

MIYAZAWA, T., KUBO, E., TAKAMURA, Y. & AKAGI, Y. 2007. Up-regulation of P-glycoprotein expression by osmotic stress in rat sugar cataract. *Exp Eye Res,* 84**,** 246-53.

MORGAN, M. J. & LIU, Z. G. 2011. Crosstalk of reactive oxygen species and NF-kappaB signaling. *Cell Res,* 21**,** 103-15.

NATOLI, M., CHRISTENSEN, J., EL-GEBALI, S., FELSANI, A. & ANDERLE, P. 2013. The role of CDX2 in Caco-2 cell differentiation. *Eur J Pharm Biopharm,* 85**,** 20-5.

NATOLI, M., LEONI, B. D., D'AGNANO, I., ZUCCO, F. & FELSANI, A. 2012. Good Caco-2 cell culture practices. *Toxicol In Vitro,* 26**,** 1243-6.

NKABYO, Y. S., ZIEGLER, T. R., GU, L. H., WATSON, W. H. & JONES, D. P. 2002. Glutathione and thioredoxin redox during differentiation in human colon epithelial (Caco-2) cells. *Am J Physiol Gastrointest Liver Physiol,* 283**,** G1352-9.

NODA, T., IWAKIRI, R., FUJIMOTO, K. & AW, T. Y. 2001. Induction of mild intracellular redox imbalance inhibits proliferation of CaCo-2 cells. *FASEB J,* 15**,** 2131-9.

OHKAWA, K., HATANO, T., ISONISHI, S., TAKADA, K., JOH, K. & MATSUDA, M. 1994. Doxorubicin enhances transient expression of p-glycoprotein and modulates activity and isoform expression of protein-kinase-C in ah66 rat hepatoma-cells. *Int J Oncol,* 4**,** 655-9.

ORCHEL, A., DZIERZEWICZ, Z., PARFINIEWICZ, B., WEGLARZ, L. & WILCZOK, T. 2005. Butyrate-induced differentiation of colon cancer cells is PKC and JNK dependent. *Dig Dis Sci,* 50**,** 490-8.

ORCHEL, A., GRUCHLIK, A., WEGLARZ, L. & DZIERZEWICZ, Z. 2006. Influence of sodium butyrate on antioxidative enzymes activity in Caco-2 cell lines. *Acta Pol Pharm,* 63**,** 441-2.

PENG, L., HE, Z., CHEN, W., HOLZMAN, I. R. & LIN, J. 2007. Effects of butyrate on intestinal barrier function in a Caco-2 cell monolayer model of intestinal barrier. *Pediatr Res,* 61**,** 37-41.

PFAFFL, M. W. 2001. A new mathematical model for relative quantification in real-time RT-PCR. *Nucleic Acids Res,* 29**,** e45.

PIANA, C., TOEGEL, S., GUELL, I., GERBES, S., VIERNSTEIN, H., WIRTH, M. & GABOR, F. 2008a. Growth surface-induced gene and protein expression patterns in Caco-2 cells. *Acta Biomater,* 4**,** 1819-26.

PIANA, C., WIRTH, M., GERBES, S., VIERNSTEIN, H., GABOR, F. & TOEGEL, S. 2008b. Validation of reference genes for qPCR studies on Caco-2 cell differentiation. *Eur J Pharm Biopharm,* 69**,** 1187-92.

RAHMAN, I., KODE, A. & BISWAS, S. K. 2006. Assay for quantitative determination of glutathione and glutathione disulfide levels using enzymatic recycling method. *Nat Protoc,* 1**,** 3159-65.

RUEMMELE, F. M., SCHWARTZ, S., SEIDMAN, E. G., DIONNE, S., LEVY, E. & LENTZE, M. J. 2003. Butyrate induced Caco-2 cell apoptosis is mediated via the mitochondrial pathway. *Gut,* 52**,** 94-100.

SAMBUY, Y., DE ANGELIS, I., RANALDI, G., SCARINO, M. L., STAMMATI, A. & ZUCCO, F. 2005. The Caco-2 cell line as a model of the intestinal barrier: influence of cell and culture-related factors on Caco-2 cell functional characteristics. *Cell Biol Toxicol,* 21**,** 1-26.

SCHAFER, F. Q. & BUETTNER, G. R. 2001. Redox environment of the cell as viewed through the redox state of the glutathione disulfide/glutathione couple. *Free Radic Biol Med,* 30**,** 1191-212.

SEVIN, E., DEHOUCK, L., FABULAS-DA COSTA, A., CECCHELLI, R., DEHOUCK, M. P., LUNDQUIST, S. & CULOT, M. 2013. Accelerated Caco-2 cell permeability model for drug discovery. *J Pharmacol Toxicol Methods,* 68**,** 334-9.

SHEN, H., XU, W., CHEN, Q., WU, Z., TANG, H. & WANG, F. 2010. Tetrandrine prevents acquired drug resistance of K562 cells through inhibition of mdr1 gene transcription. *J Cancer Res Clin Oncol,* 136**,** 659-65.

SHEN, Y., CHU, Y., YANG, Y. & WANG, Z. 2012. Mitochondrial localization of P-glycoprotein in the human breast cancer cell line MCF-7/ADM and its functional characterization. *Oncol Rep,* 27**,** 1535-40.

SHIRASAKA, Y., KONISHI, R., FUNAMI, N., KADOWAKI, Y., NAGAI, Y., SAKAEDA, T. & YAMASHITA, S. 2009. Expression levels of human P-glycoprotein in in vitro cell lines: correlation between mRNA and protein levels for P-glycoprotein expressed in cells. *Biopharm Drug Dispos,* 30**,** 149-52.

SHIRASAKA, Y., SAKANE, T. & YAMASHITA, S. 2008. Effect of P-glycoprotein expression levels on the concentration-dependent permeability of drugs to the cell membrane. *J Pharm Sci,* 97**,** 553-65.

SIISSALO, S., LAITINEN, L., KOLJONEN, M., VELLONEN, K. S., KORTEJARVI, H., URTTI, A., HIRVONEN, J. & KAUKONEN, A. M. 2007. Effect of cell differentiation and passage number on the expression of efflux proteins in wild type and vinblastine-induced Caco-2 cell lines. *Eur J Pharm Biopharm,* 67**,** 548-54.

SILVA, R., CARMO, H., DINIS-OLIVEIRA, R., CORDEIRO-DA-SILVA, A., LIMA, S. C., CARVALHO, F., BASTOS MDE, L. & REMIAO, F. 2011. In vitro study of P-glycoprotein induction as an antidotal pathway to prevent cytotoxicity in Caco-2 cells. *Arch Toxicol,* 85**,** 315-26.

SUNDSETH, R., MACDONALD, G., TING, J. & KING, A. C. 1997. DNA elements recognizing NF-Y and Sp1 regulate the human multidrug-resistance gene promoter. *Mol Pharmacol,* 51**,** 963-71.

SZAFLARSKI, W., SUJKA-KORDOWSKA, P., JANUCHOWSKI, R., WOJTOWICZ, K., ANDRZEJEWSKA, M., NOWICKI, M. & ZABEL, M. 2013. Nuclear localization of P-glycoprotein is responsible for protection of the nucleus from doxorubicin in the resistant LoVo cell line. *Biomed Pharmacother,* 67**,** 497-502.

TAKARA, K., HAYASHI, R., KOKUFU, M., YAMAMOTO, K., KITADA, N., OHNISHI, N. & YOKOYAMA, T. 2009. Effects of nonsteroidal anti-inflammatory drugs on the expression and function of P-glycoprotein/MDR1 in Caco-2 cells. *Drug Chem Toxicol,* 32**,** 332-7.

TERADA, Y., OGURA, J., TSUJIMOTO, T., KUWAYAMA, K., KOIZUMI, T., SASAKI, S., MARUYAMA, H., KOBAYASHI, M., YAMAGUCHI, H. & ISEKI, K. 2014. Intestinal P-glycoprotein expression is multimodally regulated by intestinal ischemia-reperfusion. *J Pharm Pharm Sci,* 17**,** 266-76.

THORN, C. F., OSHIRO, C., MARSH, S., HERNANDEZ-BOUSSARD, T., MCLEOD, H., KLEIN, T. E. & ALTMAN, R. B. 2011. Doxorubicin pathways: pharmacodynamics and adverse effects. *Pharmacogenet Genomics,* 21**,** 440-6.

VILABOA, N. E., GALAN, A., TROYANO, A., DE BLAS, E. & ALLER, P. 2000. Regulation of multidrug resistance 1 (MDR1)/P-glycoprotein gene expression and activity by heat-shock transcription factor 1 (HSF1). *J Biol Chem,* 275**,** 24970-6.

VREEBURG, R. A., BASTIAAN-NET, S. & MES, J. J. 2011. Normalization genes for quantitative RT-PCR in differentiated Caco-2 cells used for food exposure studies. *Food Funct,* 2**,** 124-9.

WANG, Y. D., CAI, N., WU, X. L., CAO, H. Z., XIE, L. L. & ZHENG, P. S. 2013. OCT4 promotes tumorigenesis and inhibits apoptosis of cervical cancer cells by miR-125b/BAK1 pathway. *Cell Death Dis,* 4**,** e760.

WARTENBERG, M., HOFFMANN, E., SCHWINDT, H., GRUNHECK, F., PETROS, J., ARNOLD, J. R., HESCHELER, J. & SAUER, H. 2005. Reactive oxygen species-linked regulation of the multidrug resistance transporter P-glycoprotein in Nox-1 overexpressing prostate tumor spheroids. *FEBS Lett,* 579**,** 4541-4549.

WARTENBERG, M., LING, F. C., SCHALLENBERG, M., BAUMER, A. T., PETRAT, K., HESCHELER, J. & SAUER, H. 2001. Down-regulation of intrinsic P-glycoprotein expression in multicellular prostate tumor spheroids by reactive oxygen species. *J Biol Chem,* 276**,** 17420-8.

WATSON, W. H., CHEN, Y. & JONES, D. P. 2003. Redox state of glutathione and thioredoxin in differentiation and apoptosis. *Biofactors,* 17**,** 307-14.

WOLTER, F. & STEIN, J. 2002. Resveratrol enhances the differentiation induced by butyrate in caco-2 colon cancer cells. *J Nutr,* 132**,** 2082-6.

YAMAGISHI, T., SAHNI, S., SHARP, D. M., ARVIND, A., JANSSON, P. J. & RICHARDSON, D. R. 2013. P-glycoprotein mediates drug resistance via a novel mechanism involving lysosomal sequestration. *J Biol Chem,* 288**,** 31761-71.

ZUKER, M. 2003. Mfold web server for nucleic acid folding and hybridization prediction. *Nucleic Acids Res,* 31**,** 3406-15.

APPENDICES

APPENDIX I

RT-qPCR VALIDATION

Quantification of mRNA level was performed by reverse transcriptase-quantitative polymerase chain reaction (RT-qPCR) which conformed to the Minimum Information for Publication of Quantitative Real-Time PCR Experiments (MIQE) guidelines (Bustin et al., 2009).

Experimental design

The RT-qPCR experiment was performed at least three independent experiments (n=3). As illustrated in Figure 27, Caco-2 cells were treated with either 0.5% DMSO (solvent control) or various non-cytotoxic concentrations of doxorubicin as three biological replicates. After treatment, cells were extracted for total RNA, treated with DNase, and reverse-transcribed into cDNA. Each cDNA sample was quantified for *ABCB1* and *GAPDH* mRNA level by qPCR as three technical replicates for each gene.

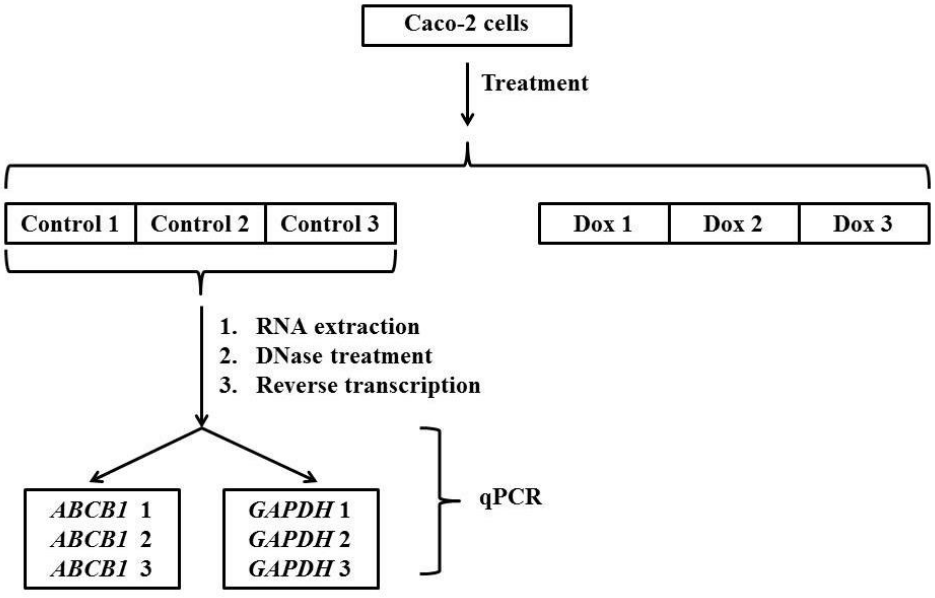

Figure 27: Experimental design of RT-qPCR assay.

Samples

In this study, samples were defined as total RNA isolated from Caco-2 cells treated with various substances as indicated.

Nucleic acid extraction

The total RNA was extracted by TRIzol reagent according to manufacturing protocol. After extraction, RNA pellets were stored in absolute ethanol at -80°C. In the day of experiment, RNA pellets were dissolved in nuclease-free water and determined concentration by Nanodrop2000 spectrophotometer. The residual DNA was digested by TURBO DNA-free kit.

RNA quality and integrity

In this study, RNA sample had good quality when nucleic acid-to-protein ratio ($A_{260/280}$) was about 1.80-2.00 and nucleic acid-to-residual solvent ratio ($A_{260/230}$) was higher than 2.00 (Figure 28).

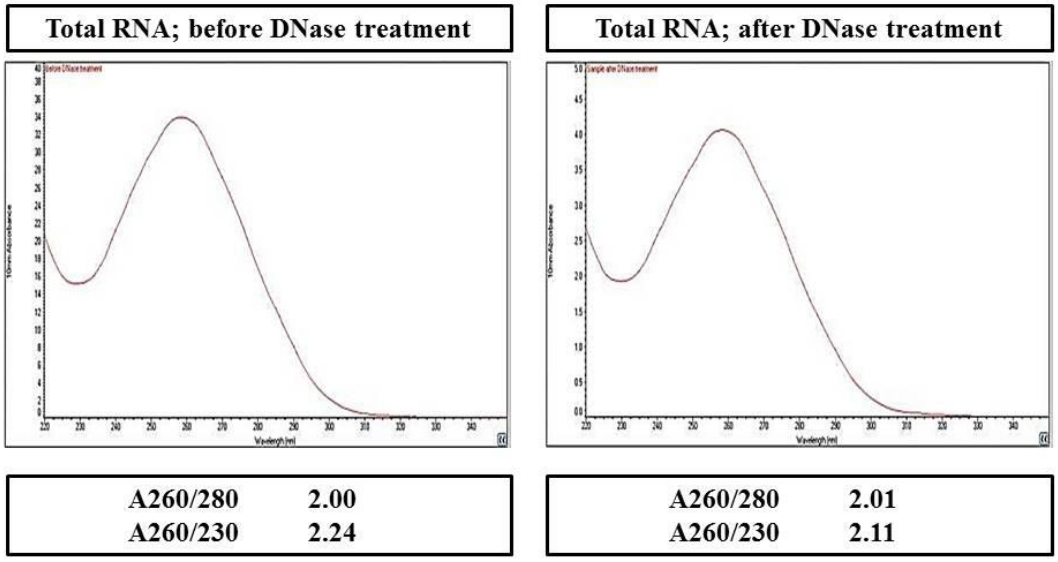

Figure 28: RNA quality of isolated total RNA before and after DNase treatment assessed by Nanodrop2000 spectrophotometer.

The RNA integrity was determined by conventional agarose gel electrophoresis method. In brief, 1.0 μg of RNA samples was separated by electrophoresis through a 1.5% agarose gel containing 1X SYBR Safe DNA gel stain.

The RNA bands were visualized by luminescent image analyzer, ImageQuant LAS4000. In this study, RNA samples had ratio of 28S:18S ribosomal RNA roughly equal to 2 and no degraded RNA (Figure 29).

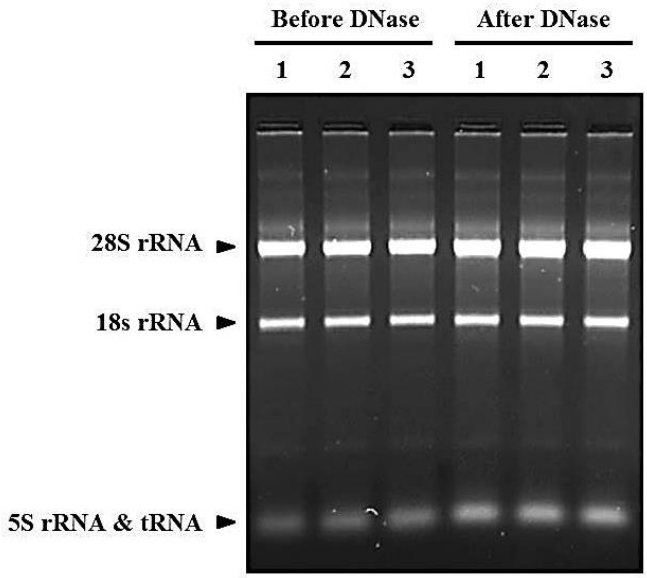

Figure 29: RNA integrity of isolated total RNA before and after DNase treatment.

Reverse transcription

The cDNA synthesis was performed using Improm-II reverse transcription system. The complete reaction mixture and reaction condition were listed in Table 2 and 3, respectively. After reverse transcription, cDNA was stored at -20°C until qPCR quantification. Notably, RT-qPCR validation was performed by 0.5 µg of DNase-treated RNA.

Table 2: The complete reaction components for cDNA synthesis

Components	Amounts
DNase-treated RNA	0.50 µg
Olido(dT)$_{15}$ primer	0.50 µg
Improm-II™ 5X reaction buffer	1:5
$MgCl_2$	2 mM
dNTP mix	0.5 mM of each
Recombinant RNasin™ inhibitor	20 U
Improm-II™ reverse transcriptase	160 U
Nuclease-free water qs to	20 µL

Table 3: The complete reaction condition for cDNA synthesis

Reaction steps	Temp. (°C)	Time (min)
RNA Denaturation	70.0	5
Annealing	25.0	5
Extension	42.0	60
Reverse transcriptase inactivation	70.0	15

qPCR target information and qPCR oligonucleotides

In this study, the reference gene was selected based on previous studies. It was reported that *GAPDH* mRNA was the least fluctuate upon Caco-2 differentiation and chemical exposure (Piana et al., 2008b, Vreeburg et al., 2011). Therefore, *ABCB1* and *GAPDH* was the gene of interest and reference gene using in this study, respectively. The sequence accession number, primer sequence, and product size were listed in Table 4. The primer location was shown in Figure 30. In addition, an *in silico* specificity was performed by NCBI database, showing that there was no unintended products (Brown et al., 2015).

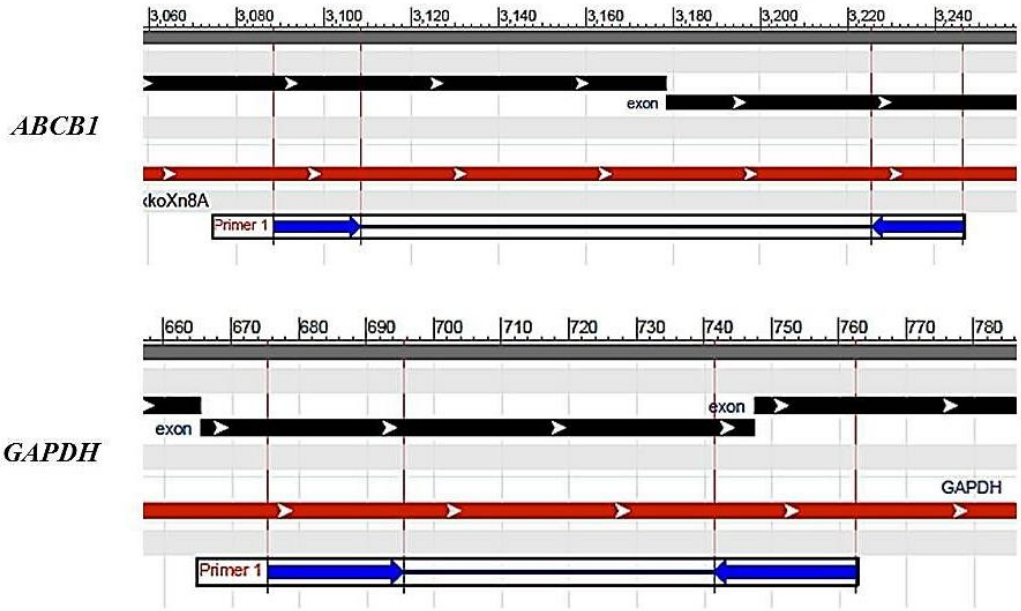

Figure 30: Location of primers used in this study.

Table 4: Sequences of primers used in this study.

Gene	Direction	Sequences (5' → 3')	Product size
ABCB1 (NM_000927.4)	Forward Reverse	CCCATCATTGCAATAGCAGG TGTTCAAACTTCTGCTCCTGA	158 bps
GAPDH (NM_001256799.2)	Forward Reverse	TGCACCACCAACTGCTTAGC GGCATGGACTGTGGTCATGAG	87 bps

qPCR protocol

The qPCR was performed by fast qPCR protocol using SsoFast Evagreen Supermixes on CFX96™ Real-Time PCR Detection System. The complete reaction mixture and thermal cycling condition were listed in Table 5 and 6, respectively. The evidences of optimization for primer concentration and annealing temperature were shown below.

Table 5: The complete reaction components for qPCR

Components	*ABCB1*	*GAPDH*
cDNA	1 µL	
Forward primer	400 nM	300 nM
Reverse primer	400 nM	300 nM
SsoFast™ Evagreen® Supermixes	1:2	
Nuclease-free water qs to	10 µL	

Table 6: The complete thermal cycling condition for qPCR

Reaction steps	Temp. (°C)	Time (sec)	Cycles
Enzyme activation	95.0	30	1
Denaturation	95.0	5	40
Annealing/Extension	60.0	5	
Melt curve	65.0 - 95.0 (in 0.5 increment)	5/step	1

Primer concentration

The concentration of primers specific to *ABCB1* and *GAPDH* genes was optimized in the range 100-500 nM in an equimolar concentration of both strands. Based on C_q values, the suitable primer concentration was selected at 400 and 300 nM for *ABCB1* and *GAPDH*, respectively (Figure 31)

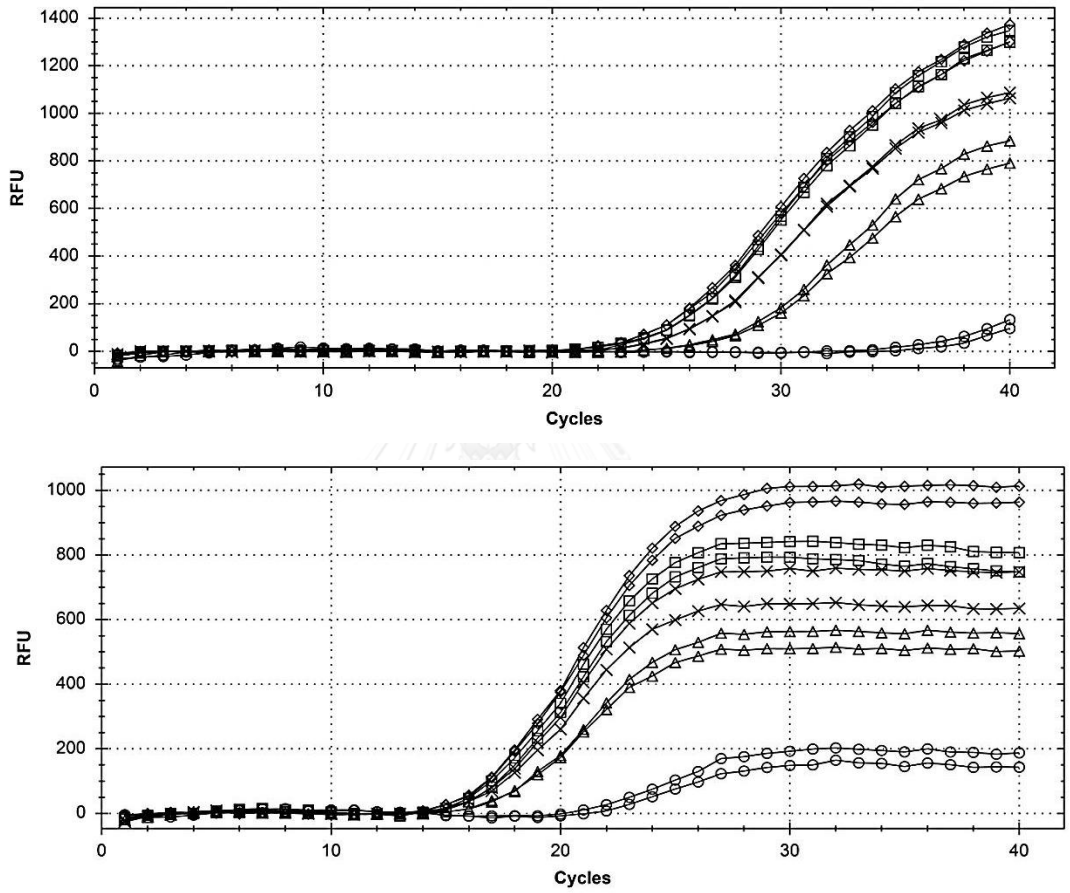

Figure 31: The amplification curve of *ABCB1* (upper) and *GAPDH* (lower) at various primer concentrations (nM): 100 (circle), 200 (triangle), 300 (cross), 400 (square), and 500 (diamond).

Annealing temperature

The annealing temperature was optimized within the gradient temperature ranging from 50.0 to 65.0°C. As shown in Table 7, the lowest C_q values of the *ABCB1* gene were obtained from annealing temperature at 59.5 and 55.9°C. In order to select one annealing temperature, the secondary structure of template was

determined by The mfold Web Server (The RNA Institute, College of Arts and Sciences State University of New York at Albany) (Zuker, 2003). As shown in Figure 32 and 33, *ABCB1* amplicon had less secondary structure at 60.0°C, but structure of *GAPDH* amplicon was similar in both temperatures. Thus, annealing temperature was set up at 60.0°C for both genes.

Table 7: The quantification cycle (C_q) from various annealing temperatures.

Annealing temperature (°C)	Quantification cycles (Cq, mean ± SD)	
	ABCB1	*GAPDH*
65.0	24.97 ± 0.037	14.83 ± 0.049
64.1	24.43 ± 0.026	14.91 ± 0.050
62.5	24.08 ± 0.001	14.92 ± 0.030
59.5	23.96 ± 0.040	15.06 ± 0.003
55.9	23.97 ± 0.012	15.42 ± 0.032
53.0	24.00 ± 0.020	15.69 ± 0.017
51.0	23.96 ± 0.006	15.86 ± 0.086
50.0	23.96 ± 0.000	15.75 ± 0.145

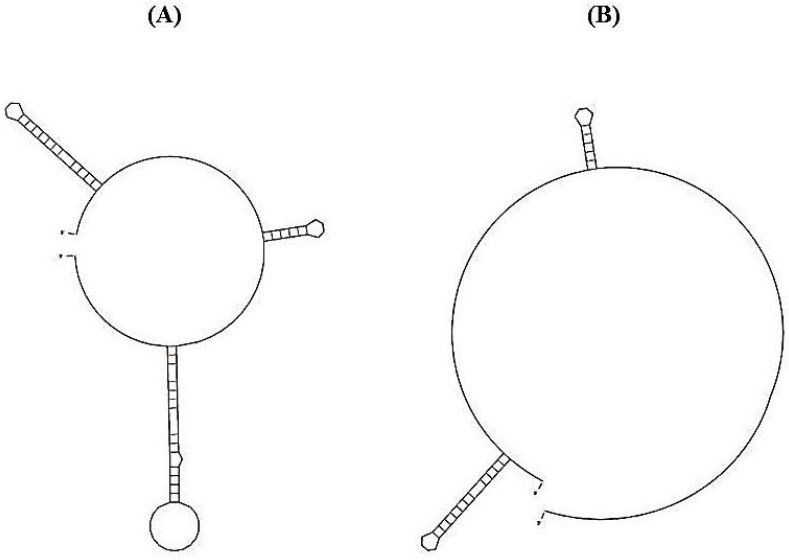

Figure 32: Secondary structure of *ABCB1* amplicon at 56.0°C (A) and 60.0°C (B).

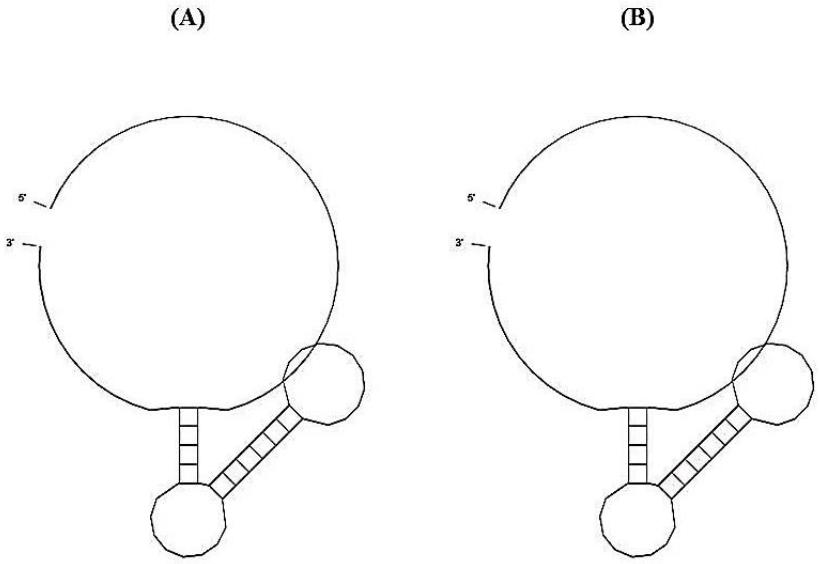

Figure 33: Secondary structure of *GAPDH* amplicon at 56.0°C (A) and 60.0°C (B).

qPCR validation

Specificity

As shown in Figure 34 and 35, amplification curves showed the specificity of qPCR in both genes. The melting temperature (T_m) of *ABCB1* and *GAPDH* amplicons was at 79.5 and 82.0°C, respectively. Neither NRT (no reverse transcription control) nor NTC (no template control) had a positive signal after 40 PCR cycles. In addition, the qPCR products showed a single intended band at 158 and 87 bps in agarose gel for *ABCB1* and *GAPDH* genes, respectively (Figure 36).

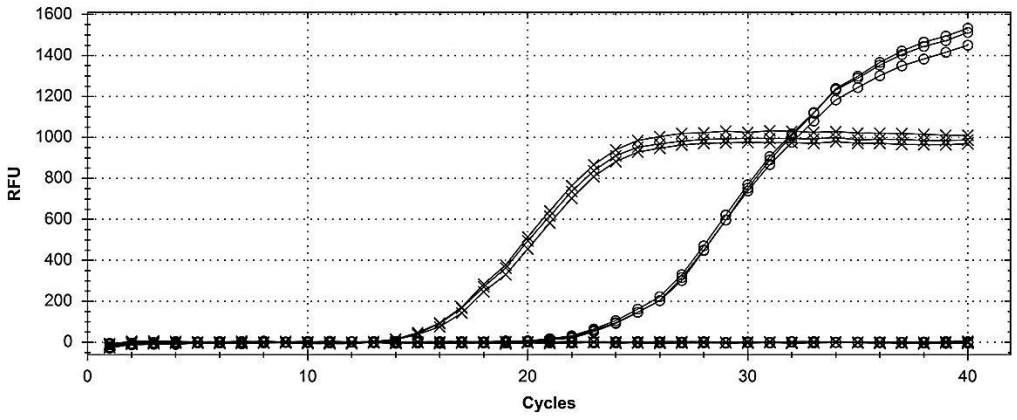

Figure 34: Amplification curve of *ABCB1* (circle) and *GAPDH* (cross) genes. The experiment was run as three technical replicates.

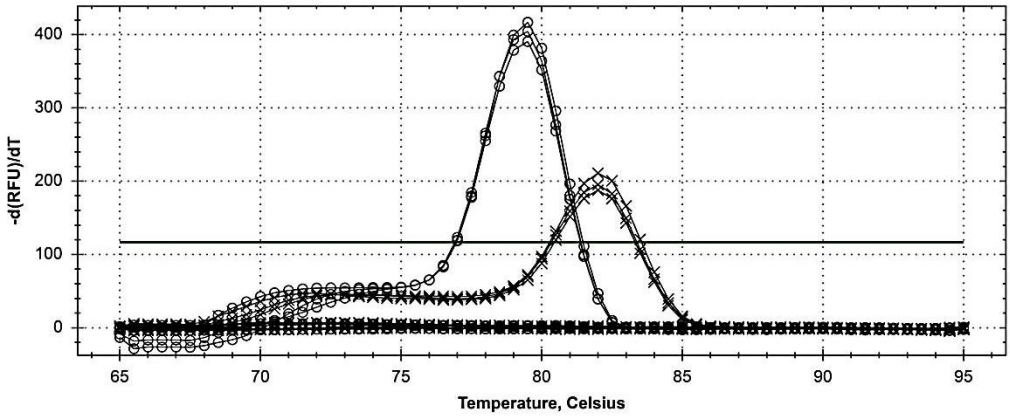

Figure 35: Melt peak of *ABCB1* (circle) and *GAPDH* (cross) genes. The experiment was run as three technical replicates.

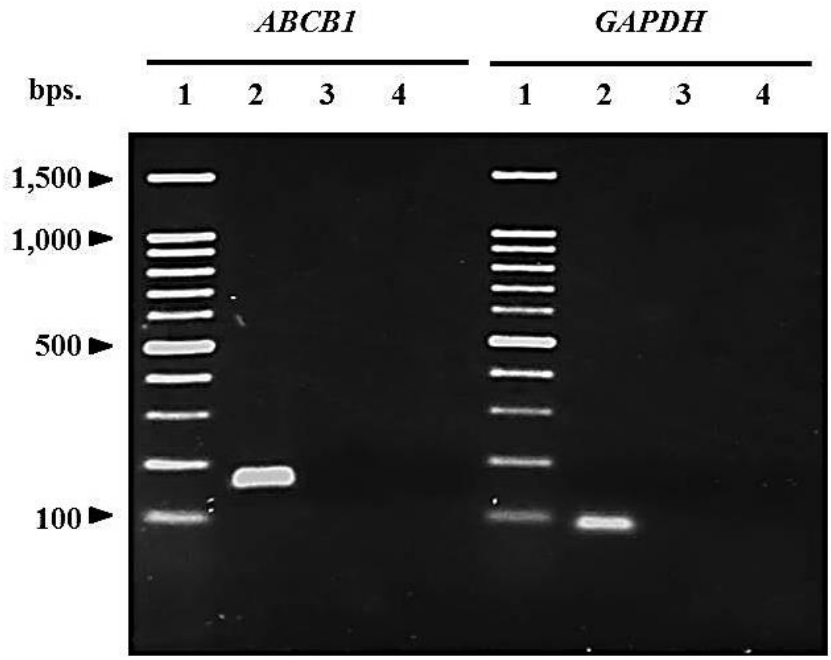

Figure 36: qPCR specificity of *ABCB1* and *GAPDH* genes in gel. The samples were loaded at 4.0 μL for each lane: DNA ladder (lane1), sample (lane2), NRT (lane3), and NTC (lane4).

Calibration curves and PCR efficiency

The standard curve was constructed from 5-fold dilution series of cDNA template (Figure 37). The slope, y-intercept, r^2, linear dynamic range, and percent of PCR efficiency were shown in Table 8. All parameters obtained from standard curve were considered to be acceptable.

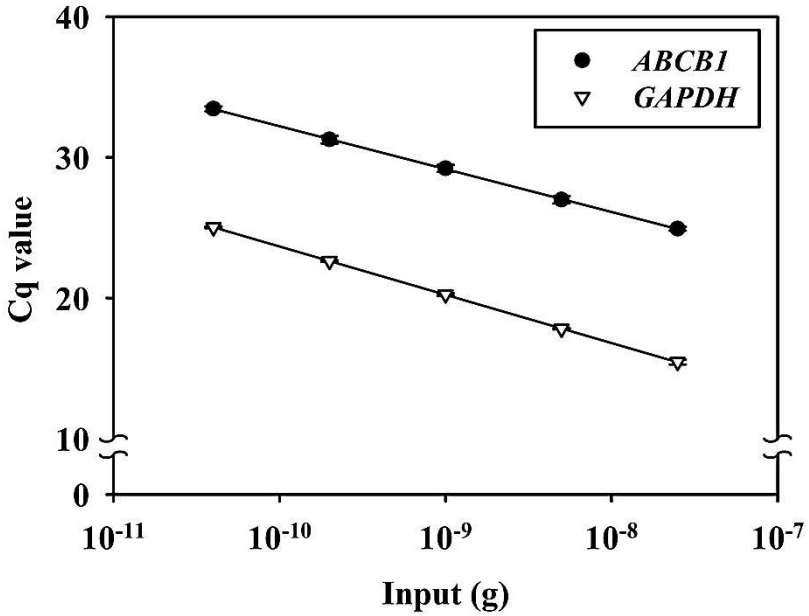

Figure 37: qPCR standard curve of *ABCB1* and *GAPDH* genes. The experiment was run as three technical replicates in three independent days. Data are expressed as mean ± SEM (n=3, triplicates).

Table 8: Validation parameter obtained from standard curve

Parameters	*ABCB1*	*GAPDH*
Slope	-3.060	-3.408
Y-intercept	1.470	-10.682
r^2	0.9998	1.0000
%PCR efficiency	112.20	96.53
Linear range	0.4 – 25.0 ng	

Repeatability and reproducibility

The repeatability (or intra-assay variation) and reproducibility (or inter-assay variation) were performed at three different inputs at 0.4, 1.0, and 25 ng. The repeatability was calculated as %CV of ten technical replicates in a single run. The reproducibility was calculated as %CV of five separated run with three technical replicates per run (Table 9).

Table 9: Repeatability and reproducibility

Genes	Input (ng)	Repeatability	Reproducibility
ABCB1	0.4	3.55	1.88
	1.0	1.97	1.66
	25.0	1.33	1.14
GAPDH	0.4	0.71	0.32
	1.0	0.89	0.57
	25.0	0.54	2.00

Normalization method

The normalization method was selected based on validated curve, constructed by plotting delta C_q against input amount (Figure 38). The simple comparative C_q method requires an assumption that slope of validated curve is approximately zero. As shown, the slope value from validated curve was 0.1682 units, which violated an assumption. Therefore, an efficiency corrected method or Pfaffl's method was used as normalization method in this study.

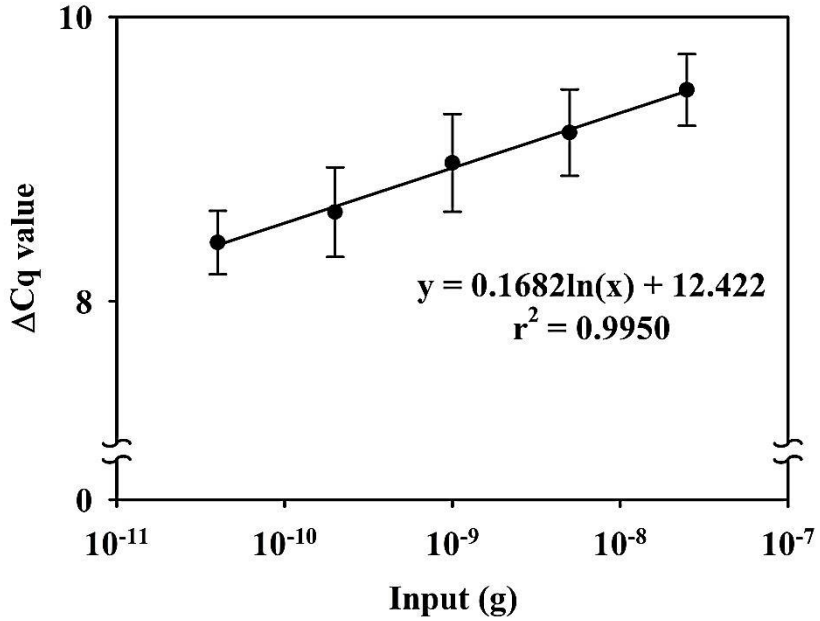

Figure 38: qPCR validated curve. The experiment was run as three technical replicates in three independent days. The delta C_q was obtained by subtraction of $C_{q,ABCB1}$ from $C_{q,GAPDH}$. Data are expressed as mean ± SEM (n=3, triplicates).

Data analysis

The data was excluded from study when they reached at least one of these criteria: nonspecific amplification, technical replicates with C_q variation > 0.5, or run with positive signals of NRT or NTC. The quantification cycle (C_q) was determined by regression model and used as an average from three technical replicates for each run. The expression ratio was calculated by efficiency corrected method and reported as mean ± SEM from at least three independent experiments, three biological replicates. The statistical analysis was performed by Mann-Whitney *U* test or Kruskal-Wallis test, where appropriate. The Bonferroni's corrected *p*-value<0.05 was considered to be statistical significance.

Limitation

The limit of detection (LOD) and limit of quantification (LOQ) were not validated in this study, because there was no sample exhibited C_q less than the lowest C_q in standard curve of each gene.

APPENDIX II

DATA SUPPLEMENTS

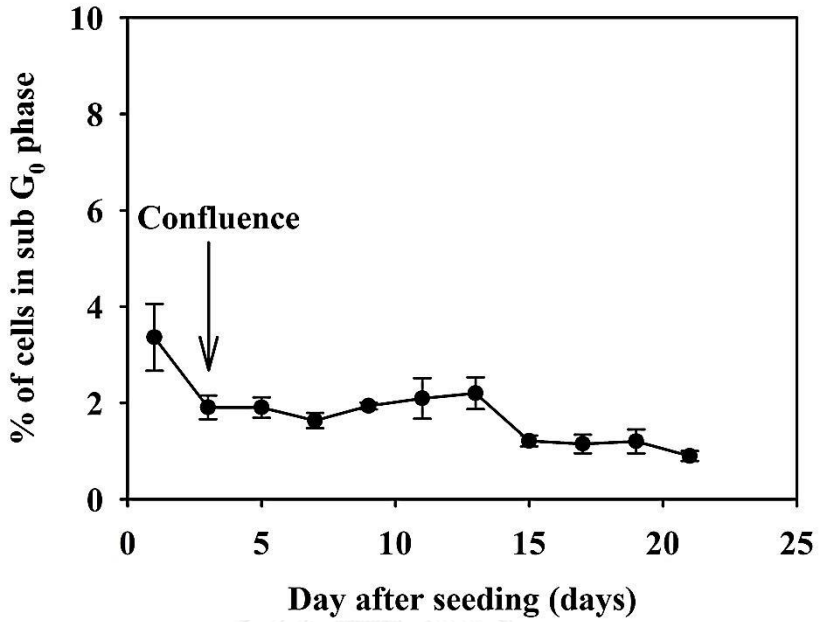

Figure 39: Percentage of Caco-2 cells in sub G_0 phase during 21-day culturing period. Data are expressed as mean ± SEM (n=3).

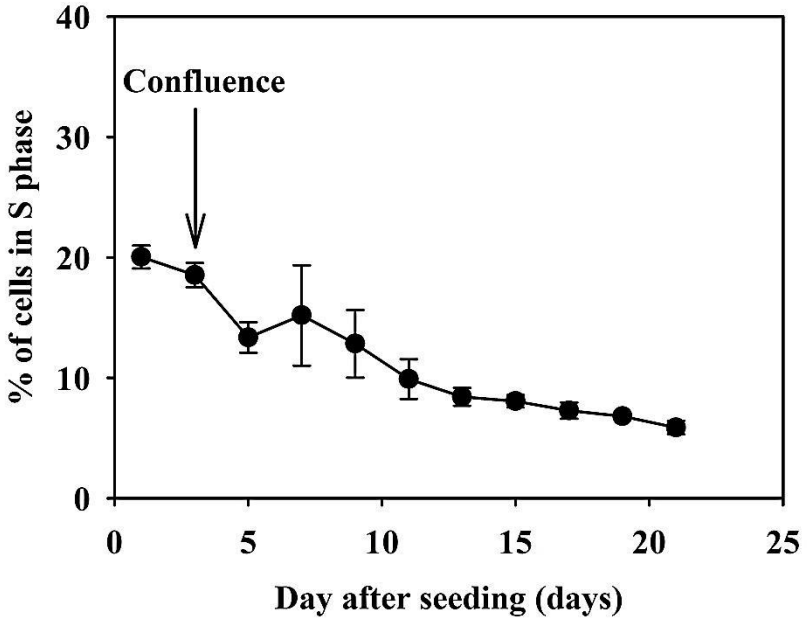

Figure 40: Percentage of Caco-2 cells in S phase during 21-day culturing period. Data are expressed as mean ± SEM (n=3).

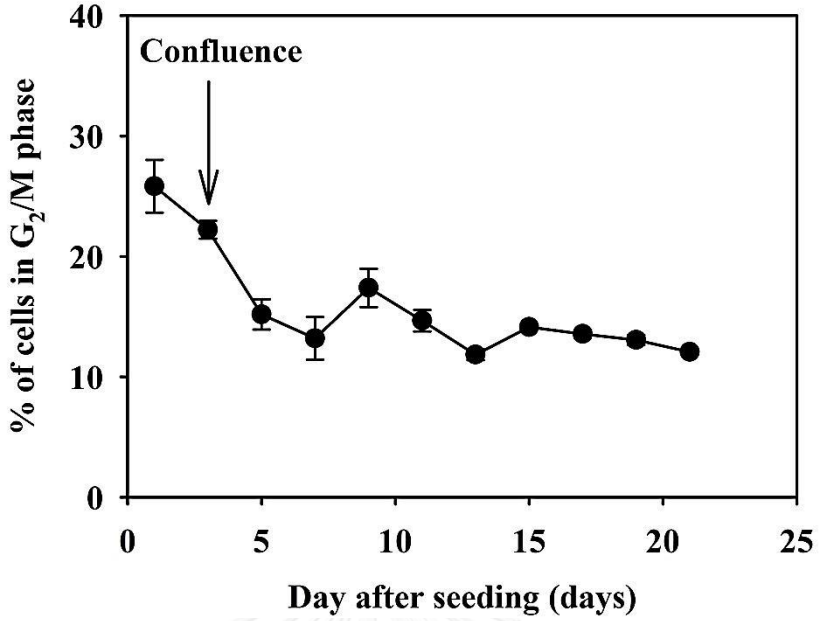

Figure 41: Percentage of Caco-2 cells in S phase during 21-day culturing period. Data are expressed as mean ± SEM (n=3).

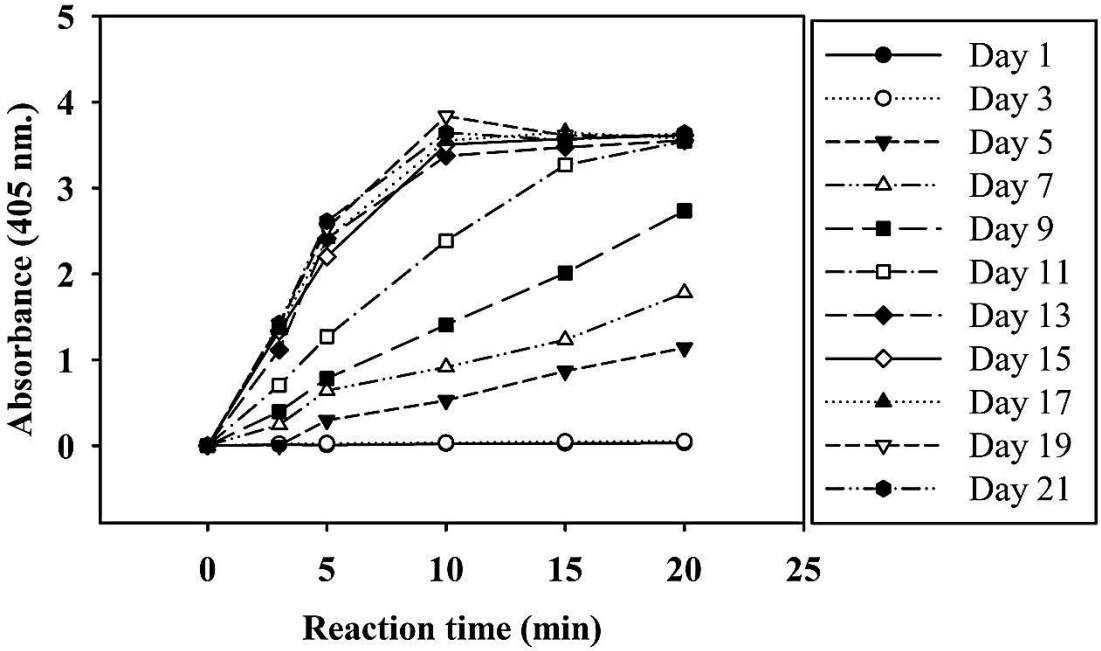

Figure 42: The rate of *p*-nitrophenol formation catalyzed by ALP enzyme from Caco-2 cells during 21-day culturing period.

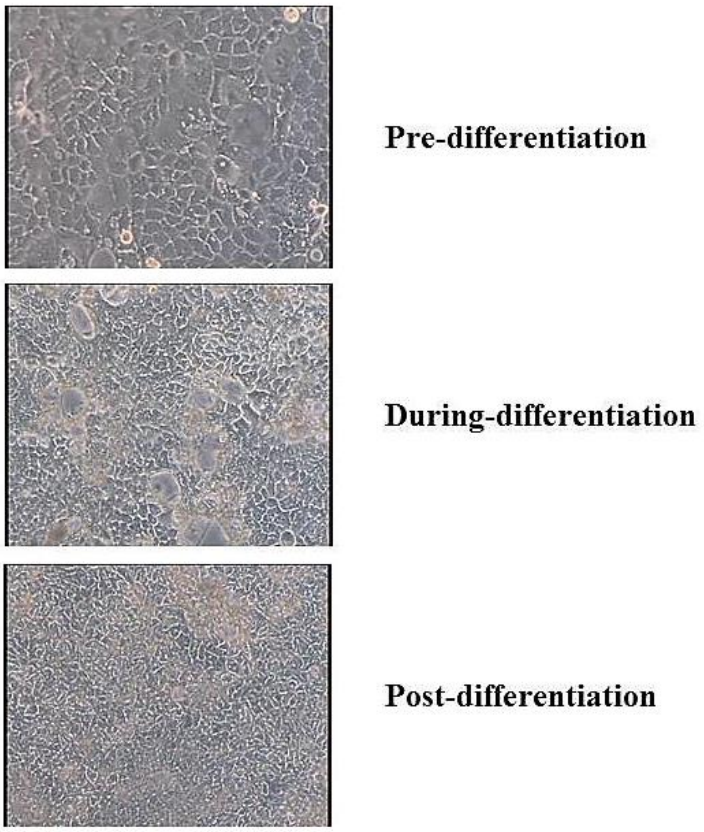

Figure 43: Morphology of Caco-2 cells at each differentiation state.

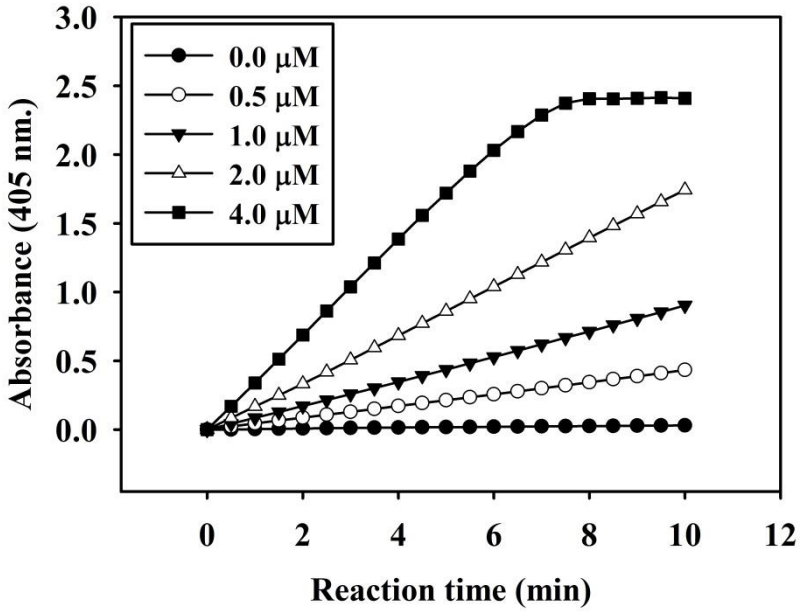

Figure 44: The rate of TNB release in enzymatic recycling assay by using standard GSSG.

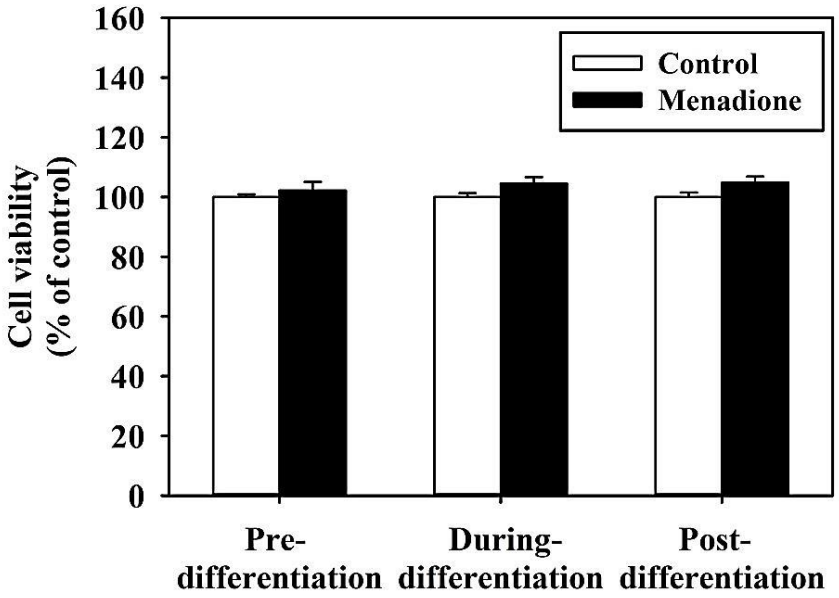

Figure 45: Effect of menadione (10 μM) on cell viability of Caco-2 cells. Data are expressed as mean ± SEM (n=3, duplicates).

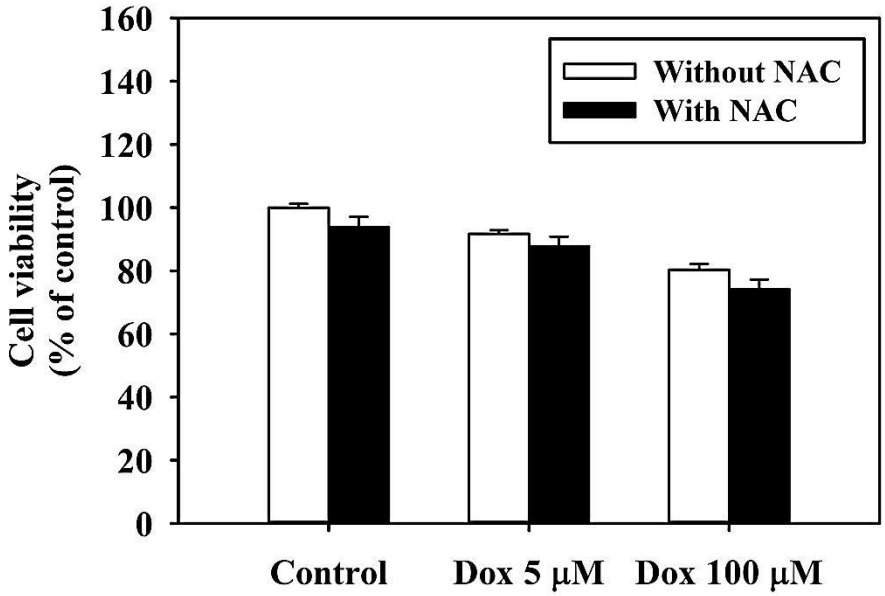

Figure 46: Effect of doxorubicin (Dox) with and without *N*-acetylcysteine (NAC) on cell viability of in the pre-differentiated Caco-2 cells. Data are expressed as mean ± SEM (n=3, duplicates).

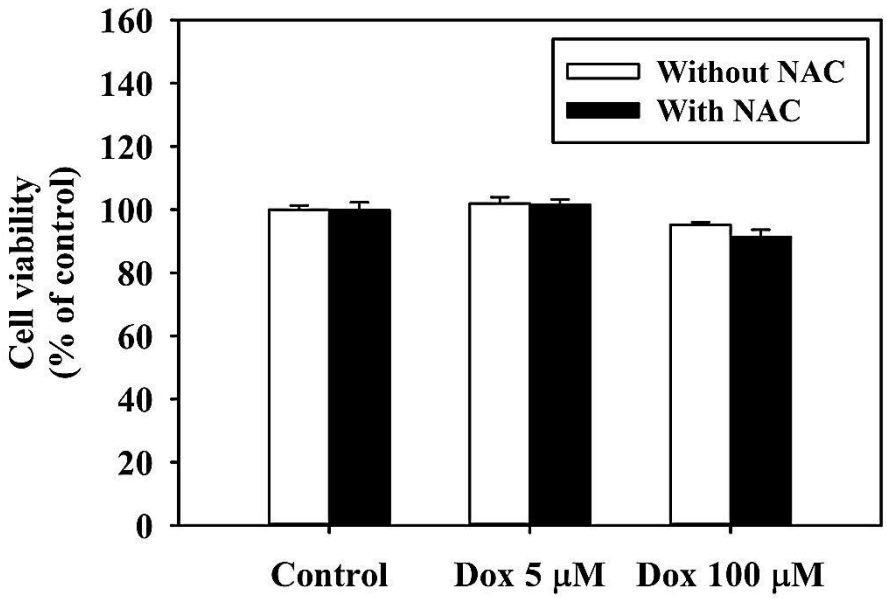

Figure 47: Effect of doxorubicin (Dox) with and without *N*-acetylcysteine (NAC) on cell viability of in the during-differentiated Caco-2 cells. Data are expressed as mean ± SEM (n=3, duplicates).

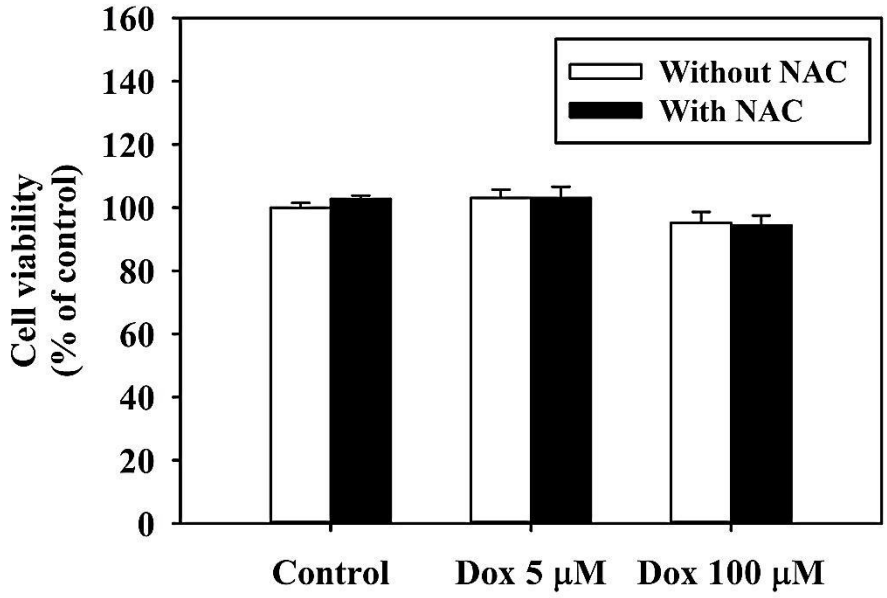

Figure 48: Effect of doxorubicin (Dox) with and without *N*-acetylcysteine (NAC) on cell viability of in the post-differentiated Caco-2 cells. Data are expressed as mean ± SEM (n=3, duplicates).

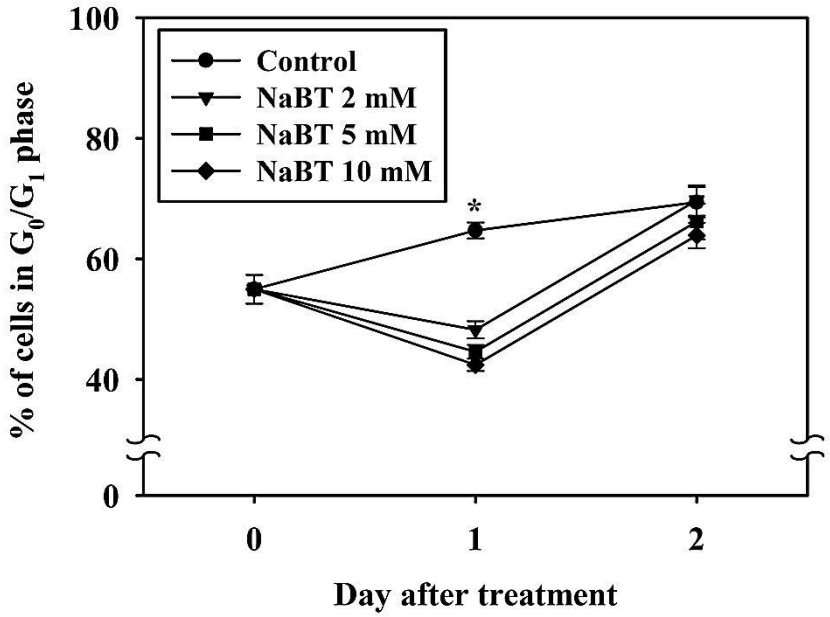

Figure 49: Effect of sodium butyrate (NaBT) on percentage of cells in G_0/G_1 phase. Data are expressed as mean ± SEM (n=3). *p<0.05 indicated statistical significance among experimental groups.

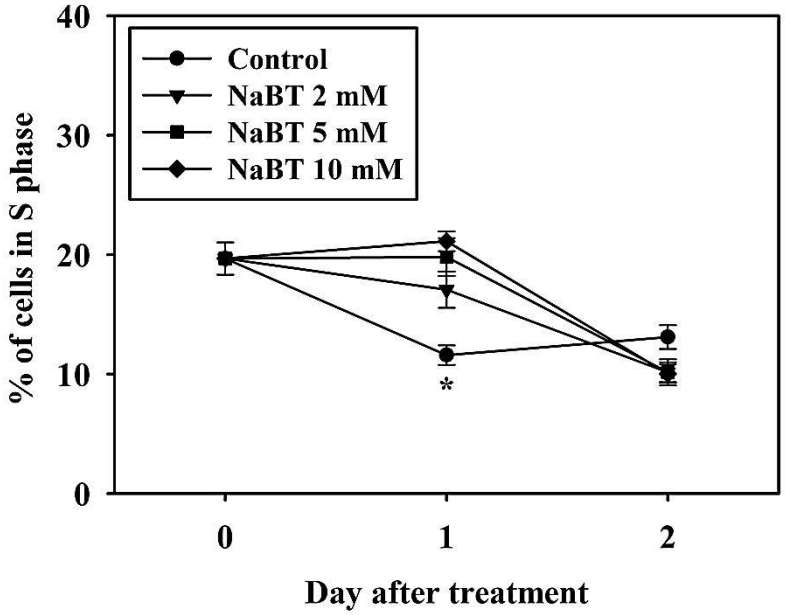

Figure 50: Effect of sodium butyrate (NaBT) on percentage of cells in S phase. Data are expressed as mean ± SEM (n=3). *p<0.05 indicated statistical significance among experimental groups.

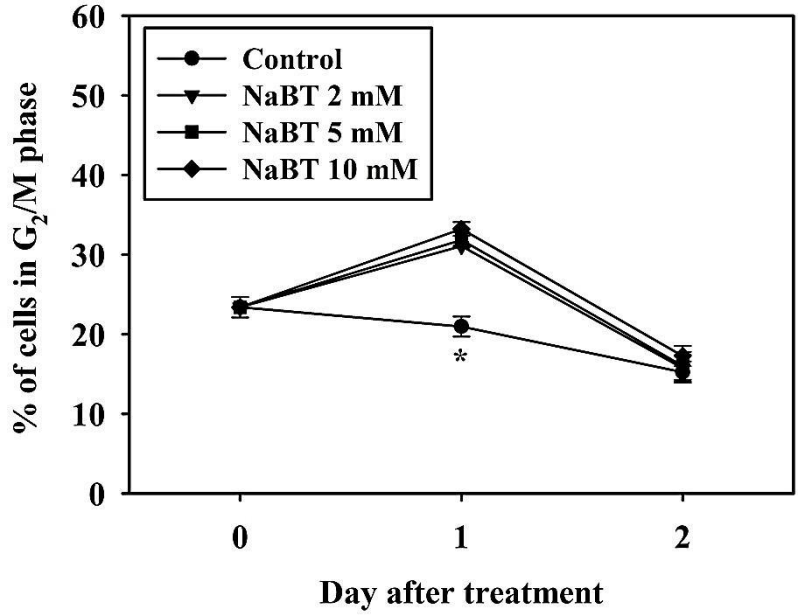

Figure 51: Effect of sodium butyrate (NaBT) on percentage of cells in G_2/M phase. Data are expressed as mean ± SEM (n=3). *p<0.05 indicated statistical significance among experimental groups.

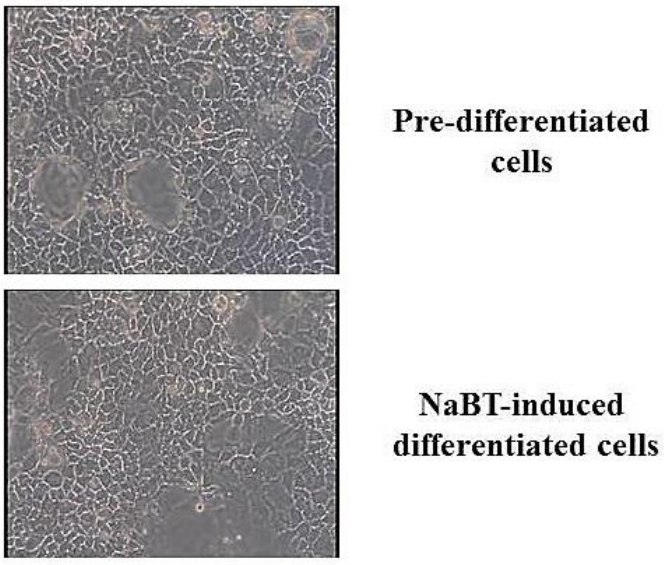

Figure 52: Morphology of the pre-differentiated cells and the NaBT-induced differentiated cells.

VITA

Mr.Udomsak Udomnilobol was born on April 3, 1990 in Bangkok, Thailand. He received the B.Sc. in Pharmacy from Faculty of Pharmaceutical Sciences, Chulalongkorn University in 2013.

During his undergraduate degree, he had a chance to work as a research assistant in two research projects about screening of Thai herbal plants for anti-advanced glycation end product activity. Both projects were under the supervision of Associate Professor Surattana Amnuoypol, Ph.D. and Associate Professor Suree Jianmongkol, Ph.D. In the last year of undergraduate life, he was interested in cardiovascular pharmacology. His senior project was in title "The inhibitory effect of hydrogen peroxide on vascular contraction of isolated rat thoracic aorta", supervised by Associate Professor Suree Jianmongkol, Ph.D.

He was granted an education scholarship "Chulalongkorn University Graduate Scholarship to Commemorate the 72th Anniversary of His Majesty King Bhumibol Adulyadej" and continued his educational life as a master degree student in pharmacology and toxicology at Faculty of Pharmaceutical Sciences, Chulalongkorn University, Bangkok, Thailand. His master's thesis was in title "The effect of doxorubicin on P-glycoprotein expression during enterocytic differentiation of Caco-2 cells", granted by The 90th Anniversary of Chulalongkorn University Fund (Ratchadaphiseksomphot Endowment Fund). Apart from his thesis, he also worked as a research assistant in the project about an interaction of P-glycoprotein and Thai medicinal plants, supervised by Associate Professor Suree Jianmongkol, Ph.D.

He was awarded as an outstanding graduate student from Chulalongkorn University in 2015.

Until 2016, he had presented the preliminary data of his master's thesis entitled "Fluorescent interference from doxorubicin in flow cytometric analysis of P-glycoprotein expression" as a poster and conference proceeding in The 13th Asia Pacific Federation of Pharmacologist (APFP) Meeting "New Paradigms in Pharmacology for Global Health" February 1st-3rd, 2016: Bangkok, Thailand.